

Authors responses to the Referees comments

Referee #1

(K. Rypdal)

GENERAL COMMENTS

Results, their relevance, and their validity

The results presented in this discussion paper are limited to assessing the linearity /non-linearity of the temperature response in two climate models, one model of intermediate complexity for the tropical Pacific (designed to describe ENSO), and one AOGCM, where the authors have confined themselves to studying results for mean northern-hemisphere land temperatures. The motivation for choice of models is not carefully explained, and their representativeness is not discussed.

The linearity issue is investigated by two methods:

(i) By considering solar, volcanic, and solar + volcanic forcing, and testing the additivity of the responses.

(ii) By testing the intermittency of the forcing and responses, assuming that in a linear system the intermittency in forcing and response should be the same. By method (i) it is found that solar and volcanic responses in the models do not add up on time scales in the range 300-1000 yr. The result is based on neglecting the estimated correlation between responses to solar and volcanic forcing, respectively (section 3.4 and Fig. 3). This approximation is justified from the statistical independence of solar and volcanic forcing. But in the model experiments these forcings are given as deterministic and do not vary over the statistical ensemble, so the estimated ensemble average over the product of these forcings is not zero. This approximation is unnecessary and may be the cause of the non-additivity result. If the authors believe it is not, they should estimate the Haar fluctuation of the sum of solar and volcanic responses directly, without using this approximation, and demonstrate that it does not change their result.

Authors: thanks for this suggestion. We implemented it (the revised fig. 3c) and it makes a little difference but doesn't change the conclusions.

Method (ii) is based on the theoretical fact that if the response is linear, the response kernel is a perfect power-law function, and the forcing is perfectly multiscaling, then the intermittency is the same for response and forcing. If the intermittencies are different the authors take it as a proof of nonlinearity of the response. However, there are at least two different tests that need to be done before one can draw this conclusion:

(a) Theoretical and estimated scaling is not the same. In order to test that the estimated intermittency is the same for the actual forcing and the response from a linear power law response model, the authors should use such a model and apply the trace-moment analysis to the response computed using this model. If the trace moments are the same as for the forcing, they can proceed to the next step.

Authors: Actually, the numerics are robust: enough tests have been done over the last thirty that we can have confidence in the trace moment technique (see e.g. [Lavallée et al., 1991] for extensive numeric tests). In actual fact, the effect here is so strong that one can detect by eye (fig. 1) the much lower "spikiness" or intermittency of the response when compared to the volcanic forcing. As indicated in the text, this was noticed over twenty years ago. Therefore we don't think that the basic result is in doubt.

(b) In this step they should question their assumption of perfect power-law scaling of the linear response. It is well known that there must be a cut-off of this response at large time scales (Rypdal and Rypdal, 2014). A cut-off at scales from a few decades to a century can easily explain the difference in intermittency. The authors should test if introduction of such a cut-off (or use of other plausible response kernels) will change the trace moments in the linear model and make them more similar to the trace moments of the actual temperature signal.

Authors: It is not at all well known that there is large scale truncation, indeed where is the evidence! All that is known is that there is a break in the scaling at some large scale between about one century and several millennia, probably depending on geographical location and epoch (see the reference in the text to the Holocene). This break is not synonymous with a truncation.

Structure and style

The paper has the form of a broad review of work by Lovejoy and co-workers, spanning most of the 16 self-citations. Most of this material is irrelevant for the interpretation of the results developed in the present paper. There is hardly a need for another review of dr. Lovejoy's work in his field in addition to the monograph Lovejoy and Schertzer, 2013. In this review I restrict myself to those aspects that are relevant for the new results presented. It does not mean that I approve of everything that is not commented.

General judgement

The manuscript is not suitable as a research article in ESD in its present form. My reservations described in points (i) and (ii) above have to be addressed and proven wrong, and a drastic shortening of the manuscript is necessary. The authors should adhere to the principles for a regular research article.

Authors: The review material was an attempt to explain the context of the problems in enough detail so that they could be understood in a fairly self-contained way. We have removed quite a lot of material in the new text and changed the structure, especially in the first part.

SPECIFIC COMMENTS

Section 1

Page 1822, lines 1-3. The comment of Blender and Fraedrich (2004) to Vyushin et al. (2004) is mentioned without discussion of its relevance. This comment discusses earlier highly relevant papers on AOGCMs.

Authors: Done

Section 2

Page 1823, lines 17-20. Here it is stated that the "ultimate goal of weather and climate modelling is to achieve $T_{sim}(t)=T_{obs}(t)$." This may be true for weather modelling within the predictability limit of about 10 days, but for weather beyond this time horizon and for climate prediction there is an inherent chaotic and unpredictable component (internal variability). It is not an "ultimate goal" to eliminate uncertainty that cannot be eliminated. A similar conceptual oddity is committed in Section 1, page 1820, line 16-23, where the authors end up stating that statistical agreement is not a sufficient condition for model validation, i.e., it is not sufficient that the model realizations and reality are shown to be independent realizations of the same stochastic process.

The authors should choose their words more carefully, since this kind of reasoning is what forms the basis of the claims of a certain group of climate change deniers who contend that GCMs are wrong because neither individual model realizations nor model ensemble means correspond to an individual observation.

Authors: Done

Section 3.1

The long passage on Page 1825, line 24 –page 1826, line 8 is very obscure, and the notation is a mess. What does expressions like mean? My guess is that $T(\Delta t)$ is a temperature fluctuation on scale Δt . But in what sense? Moving average? Haar fluctuation? What does then $T(t+\Delta t)$ mean? Again my guess is that the correct notation is to write $T(t; \Delta t)$ and $T(t+\Delta t; \Delta t)$. But if this is the Haar fluctuation, what does then the difference $\Delta T(\Delta t) = T(t+\Delta t) - T(t)$ mean? The Haar fluctuation is already a difference, so this is then a difference of differences? And what is the relevance of writing up the expression for the variance of $\Delta T(\Delta t)$?

The last sentence, “. . .fluctuations at scale Δt are no longer determined by frequencies $1/\Delta t$ but rather by irrelevant low frequency detail of the empirical sample,” seems wrong. Isn't it the other way around? I think the entire passage could be replaced by the sentence: For $H < 0$ the high-frequency details dominate the differences and prevent these differences to decrease with increasing scale Δt .

Authors: Done

Section 3.2

The discussion of statistical uncertainty in long-range dependent processes concludes that an explicit stochastic model is needed to obtain numerical realisations (Monte Carlo simulations). I agree with that. But then the authors write: "However, it is not the aim of this paper and thus it has not been done here." This is a very strange statement since the Haar fluctuation is plotted in five out of six figures for all scales up to the length of the data record. For the longest scales the statistical uncertainty is huge, and cannot be ignored "because it is not the aim of the paper." I haven't found a decent discussion of this uncertainty in any of Lovejoy's papers, so this point could be relevant to treat here.

The authors then proceed to a lengthy description of what they call "stochastic uncertainty." From their description I cannot find any difference between the statistical uncertainty that requires stochastic models and this stochastic uncertainty. This should be clarified.

Authors: Done

Section 3.4

In the text the authors again do not define the meaning of $\Delta T(\Delta t)$, but in the caption of Fig. 3 it is written that that one is plotting the RMS Haar fluctuation, so as a working hypothesis I assume that $\Delta T(\Delta t)$ is the Haar fluctuation on scale Δt , at time t . On line Page 1834, line 18 it is assumed that $\Delta T(\Delta t) = 0$, justified by the independence of the solar and volcanic forcing. The first thing is that I don't understand why it is necessary to make this approximation at all. Why not compute the RMS of the Haar fluctuation given in Eq. (4) directly? The second is that the neglect of is highly

questionable. The symbol $\langle \dots \rangle$ denotes ensemble average over 100 realisations of the ZC model. The responses $\Delta T_s(\Delta t)$ and $\Delta T_v(\Delta t)$ are strongly correlated with the forcings F_s and F_v respectively. But in the simulations these forces are deterministic, i.e., they are the same in all realisations in the ensemble. So even if it were true that the deterministic component of the responses were proportional to the forcings, such that $\sim F_s(\Delta t) F_v(\Delta t)$, the product of the forcings is not zero. As mentioned in the general comments, the authors must find a way to demonstrate the validity of this approximation, or estimate the Haar fluctuation of the sum of solar and volcanic responses directly. The latter is just as easy computationally.

Authors: Done

Page 1836, lines 16-18. Here the authors comment on Fig. 4, and write: "Since the ZC model (including volcanic forcing) has nearly the same statistics (as GISS), we may conclude that the combined solar and volcanic forcing is also quite weak." I don't understand this conclusion. The forcing is given in Fig. 1. We know what it is. Maybe the authors mean the combined response? But weak compared to what? We are comparing apples and oranges; an intermediate complexity model for ENSO (tropical Pacific) with a GCM result for northern hemisphere land. I don't get the message from this figure.

Authors: corrected -done

Page 1836, lines 20-24 and Fig 4. The slope of the fluctuation function of the control run is supposed to imply something about "the convergence of the control to the model climate." I don't understand. What convergence? What is the "model climate?"

Fig. 4. The multiproxies have high fluctuations on scales < 100 yr. This is associated with the warming since the little ice age (LIA), and contains an anthropogenic contribution. The last millennium GISS E-2-R simulation apparently exhibits a weak LIA, but this is not the case with several other AOGCM experiments over the last millennium (Østvang et al., 2014). How representative is the GISS E-2-R?

Authors: corrected -done

TECHNICAL CORRECTIONS

Page 1852, line 17. The reference to Vyshin et al. is incomplete.

Figure 1. Panel b and c, use yr BP on the horizontal axis rather than date.

Figure 2b. Top and bottom are inconsistent between figure and caption.

Figure 3 (a). The curves for multiproxies are missing. Caption, lines 3 and 4. Fig. 2b and 2b should be 3a and 3b.

Figure 6 The lines between the red points should be red, or at least a different color from the regression lines. Why are the regression lines wiggly? (a), (b), (c) are used to label panels and also to enumerate a list in the caption. Very confusing.

Authors: Technical corrections: corrected -done

Anonymous Referee #2

General comments

This manuscript studied the linear and nonlinear responses of last millennium climate models to volcanic and solar forcings. By testing i) the additivity and ii) the intermittency of the responses, the authors found i) additivity of the radiative forcings works up until roughly 50 year scales; and ii) the volcanic intermittency was much stronger than the solar intermittency, but the model responses were not very sensitive. Therefore, an important conclusion was reached, that is, linear stochastic models may be valid from over most of the macroweather range, from about 10 days to over 50 years. This study is new, and the conclusion is important. Therefore, I would like to recommend publishing this manuscript in Earth System Dynamics after a minor revision.

Authors: We thank the referee for his positive evaluation and useful comments.

Specific comments:

1. The paper is not well structured. In the current manuscript, there are “1 Introduction”, “2 Data and analysis”, “3 Method”, “4 Intermittency: multifractal trace moment analysis”, and “5 conclusion” five sections. The main results are shown in “3 Method”, and “4 Intermittency: multifractal trace moment analysis”. But you still can find some method description in “4 Intermittency: multifractal trace moment analysis”. When reading the manuscript, one may easily get lost. Therefore, I suggest the authors to improve the paper structure, such as i) add a new section as “Results”, and move the results shown in “3 Method” and “4 Intermittency: multifractal trace moment analysis” into the newly added “Results” section; ii) move the subsection “4.1 The Trace moment analysis technique” into the “Method” section, etc.
2. The scientific idea, as well as the results, are not well explained. The authors spent too much energy in reviewing other works, which seems to be too much in details, and not so relevant. Therefore, I would like to suggest the authors to shorten the paper and make it more compact. Some less relevant introductions can be put into supplementary materials.
3. In the introduction, the authors summarized the scaling regimes of different time scales. They claim that the scaling behaviors is changeable. The “macroweather” regime (>10 days, $H < 0$) can continue to time scales of 10-30 years (industrial) and 50-100 years (pre-industrial), after which a new $H > 0$ regime is observed. They further introduce that the scaling picture has recently been extended to “macroclimate” ($H < 0$, from about 80 to 500 kyr) and “megaclimate” regimes ($H > 0$, from 500 kyr to at least 500 Myr). However, these results are based on the GCM control runs and paleotemperature proxies, which may bring us with big uncertainties, or even biased scaling behaviors. I am not saying the changing scaling behaviors are incorrect, but one may need to be more careful when drawing a conclusion based on GCM control runs and paleotemperature proxies. Therefore, I would like to suggest the authors to at least mention the possible uncertainties (or even biases) in the GCM runs and paleotemperature proxies.

Authors: We have removed the old section 3.2 and other review material that was not essential to our point. We have tightened up the introduction and given it more structure, and have made numerous other changes to improve the ms. Based on the referee's comments.

Technical corrections:

4. On page 1827, line 28, and on page 1828, line 1, the authors mentioned “Figure 2b (left)” and “Figure 2b (right)”. Unfortunately, I cannot find in Figure 2b a left subfigure, nor a right

subfigure. I guess it should be “Figure 2b (top)” and “Figure 2b (bottom)”.

5. On page 1857, Figure 3a, the curve for “Multi-Proxies 1500-1900” is missing.

6. On page 1858, in the caption of Figure 3, it is confusing that there are surprisingly one sentence describing Figure 2. Line 3-4, “: : Fig.2b left, “spliced” with a 10Be reconstruction with a 40 yr smoother, Fig. 2b right): : :” This sentence should be removed.

Authors: Technical corrections: corrected -done

Anonymous Referee #3

The authors analysis output from millennium experiments with the Zebiac-Cane model and the GISS model. They conclude that both models underestimate variability at centennial scaled compared to observations, and also observe a phenomenon of 'subadditivity' in the ZC model.

(1) One of the surprising findings featured in this article is the 'subadditivity' of the Zebiac-Cane model. When it is forced by both solar and volcanic forcings, the ZC model has a spectrum response close to the simulations with volcanic forcing only, as if the solar forcing had been ignored. The seasoned modeller would be tempted to attribute the result to a trivial mistake in the experiment design. Assuming that chances of mistakes have been checked and eliminated, we need to find an explanation to this result and discuss wisely its implications for our understanding of climate dynamics. We remember that the ZC model was developed specifically to study tropical Pacific interannual variability, and in particular the ENSO phenomenon. It does not have deep ocean dynamics, nor extratropical atmospheric dynamics, which are two processes which may significantly interplay with interdecadal variability. Lacking ocean modes of motions active at times scales over a few years, the use of the ZC model in a study focused on long-memory processes and non-linearity at time scales of several hundreds of years is highly contentious.

The inadequacy of the ZC model for spectral analysis at scales over decades is a case for rebuttal of the article.

Authors' response:

We agree that the ZC model is not the theoretically optimal model for this problem. However, as we indicated, there are no equivalent suites of models that are better: no Millenium simulations exist with the necessary suite of: solar, volcanic, solar plus volcanic simulations.

That being said, there are clearly sources of low frequency variability present in the ZC model. For example, using 360 year control runs, [Goswami and Shukla, 1991] showed that due to its internal variability, that the ZC model can generate very significant multidecadal and centennial low frequency variability due to the feedbacks between SST anomalies, low level convergence and atmospheric heating. In justifying his Millenium ZC simulations, Mann specifically cited model centennial scale variability as a motivating factor. Therefore, it isn't perhaps so surprising that we find sub-additivity at scales ≈ 50 years and longer, although we agree that the conclusions are not so strong on this point, and the source of the nonlinearity in the models needs to be pin-pointed.

References

Goswami, B. N., and J. Shukla (1991), Aperiodic Variability in the Cane—Zebiak Model, *J. of Climate*, 6, 628-638.

Lavallée, D., S. Lovejoy, and D. Schertzer (1991), On the determination of the codimension function, in Non-linear variability in geophysics: Scaling and Fractals, edited by D. Schertzer and S. Lovejoy, pp. 99-110, Kluwer.

Scaling regimes and linear / nonlinear responses of last millennium climate to volcanic and solar forcings

S. Lovejoy¹, and C. Varotsos²

¹Physics, McGill University, 3600 University St., Montreal, Que., Canada

²Climate Research Group, Division of Environmental Physics and Meteorology, Faculty of Physics, University of Athens, University Campus Bldg. Phys. V, Athens 15784, Greece

Correspondence to: S. Lovejoy (lovejoy@physics.mcgill.ca) and C. Varotsos (covar@phys.uoa.gr)

Abstract. At scales much longer than the deterministic predictability limits (about 10 days), the statistics of the atmosphere undergoes a drastic transition, the high frequency weather acts as a random forcing on the lower frequency macroweather. In addition, up to decadal and centennial scales the equivalent radiative forcings of solar, volcanic and anthropogenic perturbations are small compared to the mean incoming solar flux. This justifies the common practice of reducing forcings to radiative equivalents (which are assumed to combine linearly), as well as the development of linear stochastic models, including for forecasting at monthly to decadal scales.

In order to clarify the validity of the linearity assumption and determine its scale range, we use last Millennium simulations, both with the simplified Zebiac- Cane (ZC) model and the NASA GISS E2-R fully coupled GCM. We systematically compare the statistical properties of solar only, volcanic only and combined solar and volcanic forcings over the range of time scales from one to 1000 years. We also compare the statistics to multiproxy temperature reconstructions. The main findings are: a) that the variability of the ZC and GCM models are too weak at centennial and longer scales, b) for longer than ≈ 50 years, the solar and volcanic forcings combine subadditively (nonlinearly) compounding the weakness of the response, c) the models display another nonlinear effect at shorter scales: their sensitivities are much higher for weak forcing than for strong forcing (their intermittencies are different) and we quantify this with statistical scaling exponents.

1. Introduction

1.1 Linearity versus nonlinearity

The GCM approach to climate modeling is based on the idea that whereas weather is an initial value problem, the climate is a boundary value problem (Bryson, 1997; Pielke, 1998). This means that although the weather's sensitive dependence on initial conditions (chaos, the "butterfly effect") leads to a loss of predictability at time scales of about 10 days, nevertheless averaging over enough "weather" leads to a convergence to the model's "climate". This climate is thus the state to which averages of model outputs converge for fixed atmospheric compositions and boundary conditions (i.e. control runs).

The question then arises as to the response of the system to small changes in the boundary conditions: for example anthropogenic forcings are less than 2 W/m², and at least over scales of several years, solar and volcanic forcings are of similar magnitude or smaller (see e.g. Fig. 1a and the quantification in Fig. 2). These numbers are of the order of 1% of the mean solar radiative flux so that we may anticipate that the atmosphere responds fairly linearly. This is indeed that usual assumption and it justifies the reduction of potentially complex forcings to overall radiative forcings (see Meehl et al., 2004) for GCM

Διαγράφηκε: Scaling regimes and Linear and Nonlinear responses of Last Millennium climate models to volcanic and solar forcings

¶
Shaun Lovejoy¹, Costas A. Varotsos²¶
1Physics, McGill University, 3600 University st., Montreal, Que., Canada¶
2Climate Research Group, Division of Environmental Physics and Meteorology, Faculty of Physics, University of Athens, University Campus Bldg. Phys. V, Athens 15784, Greece

-----Αλλαγή σελίδας-----
¶

Διαγράφηκε: L

Διαγράφηκε: and

Διαγράφηκε: N

Διαγράφηκε: L

Διαγράφηκε: M

Διαγράφηκε: ¶

Διαγράφηκε: models

Διαγράφηκε: haun

Διαγράφηκε: ostas A.

Διαγράφηκε: *

Διαγράφηκε: ¶

¶

Διαγράφηκε: Abstract¶

Διαγράφηκε: of validity

Διαγράφηκε:

Διαγράφηκε:

Διαγράφηκε: 1.

Διαγράφηκε: :

Διαγράφηκε: ¶

Διαγράφηκε: f

Διαγράφηκε: f

34 investigations at annual scales and [Hansen et al., \(2005\)](#) for Greenhouse gases. However, at long enough scales, linearity
 35 clearly breaks down, indeed starting with the celebrated “Daisy world” model ([Watson and Lovelock, 1983](#)), there is a whole
 36 literature that uses energy balance models to study the strongly nonlinear interactions/feedbacks between global temperatures
 37 and albedoes. There is no debate that temperature-albedo feedbacks are important at the multimillennial scales of the glacial-
 38 interglacial transitions. While some authors (e.g. [Roques et al., 2014](#)) use time scales as short as 200 years for the critical ice-
 39 albedo feedbacks, others have assumed that the temperature response to solar and volcanic forcings over the last millennium are
 40 reasonably linear (e.g. [Østvand et al., 2014](#); [Rypdal and Rypdal, 2014](#)) while [Pelletier, \(1998\)](#) and [Fraedrich et al., \(2009\)](#) assume
 41 linearity to even longer scales.

42 It is therefore important to establish the times scales over which linear responses are a reasonable assumption. However,
 43 clearly even over scales where typical responses to small forcings are relatively linear, the response may be nonlinear if the
 44 forcing is – volcanic or volcanic- like i.e. if it is sufficiently “spikey” or intermittent.

45 **1.2 Atmospheric variability: scaling regimes**

46 Before turning our attention to models, what can we learn empirically? Certainly, at high enough frequencies (the weather
 47 regime), the atmosphere is highly nonlinear. However, at about ten days, the atmosphere undergoes a drastic transition to a lower
 48 frequency regime, and this “macroweather” regime is potentially quasi- linear in its responses. Indeed, the basic atmospheric
 49 scaling regimes were identified some time ago - primarily using spectral analysis ([Lovejoy and Schertzer, 1986](#); [Pelletier, 1998](#);
 50 [Shackleton and Imbrie, 1990](#); [Huybers and Curry, 2006](#)). However, the use of real space fluctuations provided a clearer picture
 51 and a simpler interpretation. It also showed that the usual view of atmospheric variability, as a sequence of narrow scale range
 52 processes (e.g. nonlinear oscillators), has seriously neglected the main source of variability, namely the scaling “background
 53 spectrum” ([Lovejoy, 2014](#)). What was found is that for virtually all atmospheric fields, there was a transition from the behavior
 54 of the mean temperature fluctuations scaling $\langle \Delta T(\Delta t) \rangle \approx \Delta t^H$ with $H > 0$ to a lower frequency scaling regime with $H < 0$ at
 55 scales $\Delta t \gtrsim 10$ days; the macroweather regime. The transition scale of around 10 days, can be theoretically predicted on the
 56 basis of the scaling of the turbulent wind due to solar forcing (via the imposed energy rate density; see [Lovejoy and Schertzer,](#)
 57 [2010](#); [Lovejoy and Schertzer, 2013](#); [Lovejoy et al., 2014](#)). Whereas the weather is naturally identified with the high frequency
 58 $H > 0$ regime and with temperature values “wandering” up and down like a drunkard’s walk, the lower frequency $H < 0$
 59 regime is characterized by fluctuations tending to cancel out – effectively starting to converge. This converging regime is a low
 60 frequency type of weather, described as “macroweather” ([Lovejoy, 2013](#); [Lovejoy et al., 2014](#)). For the GCM control runs,
 61 macroweather effectively continues to asymptotically long times; in the real world, it continues to time scales of 10-30 years
 62 (industrial) and 50-100 years (pre-industrial) after which a new $H > 0$ regime is observed: it is natural to associate this new
 63 regime with the climate (see [Fig. 5 of Lovejoy et al., 2013](#); see also [Franzke et al., 2013](#)). Other papers analyzing macroweather
 64 scaling include [Koscielny-Bunde et al., \(1998\)](#); [Eichner et al., \(2003\)](#); [Kantelhardt et al., \(2006\)](#); [Rybski et al., \(2006\)](#); [Bunde et](#)
 65 [al., \(2005\)](#); [Østvand et al., \(2014\)](#); [Rypdal and Rypdal, \(2014\)](#).

66 The explanation for the “macroweather” to climate transition (at scale τ_c) appears to be that over the “macroweather” time
 67 scales - where the fluctuations are “cancelling” - other, slow processes which presumably include both external climate forcings
 68 and other slow (internal) land-ice or biogeochemical processes – become stronger and stronger. At some point (τ_c) their

Διαγράφηκε: [...]...[...]
 [...]...[...],...,...[...],...and...[...]
]...; (... [1])

Διαγράφηκε: ¶

Διαγράφηκε: T

Αλλαγή κωδικού πεδίου

Διαγράφηκε: [...]...[...]
 [...]...[...],...,...[...],...and...[...]
]...; (... [2])

Διαγράφηκε: $\langle \Delta T(\Delta t) \rangle \approx \Delta t^H$...
 $H > 0$ (... [3])

Διαγράφηκε:

Διαγράφηκε: $H < 0$...[... [4]

Διαγράφηκε: at...with the
 latter time scale being (... [5])

Διαγράφηκε: [

Αλλαγή κωδικού πεδίου

Διαγράφηκε:]...[(... [6])

Αλλαγή κωδικού πεδίου

Διαγράφηκε:]

Διαγράφηκε: $H > 0$...[... [7]

Διαγράφηκε: [

Αλλαγή κωδικού πεδίου

Διαγράφηκε:]...[(... [8])

Αλλαγή κωδικού πεδίου

Διαγράφηκε:]

Διαγράφηκε: $H > 0$

Διαγράφηκε:

Διαγράφηκε: f...[(... [9])

Αλλαγή κωδικού πεδίου

Διαγράφηκε:]...[(... [10])

Αλλαγή κωδικού πεδίου

Διαγράφηκε:]...[(... [11])

Αλλαγή κωδικού πεδίου

Διαγράφηκε:]...[(... [12])

Αλλαγή κωδικού πεδίου

Διαγράφηκε:]

Διαγράφηκε: τ_c

variability dominates., from ≈ 80 kyrs to ≈ 500 kyrs) and “megaclimate” regimes ($H > 0$, from 500 kyrs to at least 550 Myrs; see A significant point where opinions diverge is the value of the global transition scale τ_c during the preindustrial Holocene; see (Lovejoy, 2015a) for a discussion.

1.3 Scaling in the numerical models

There have been several studies of the low frequency control run responses of GCMs (Vyushin et al., 2004; Zhu et al., 2006; Fraedrich et al., 2009; Lovejoy et al., 2013) finding that they are scaling down to their lowest frequencies. This scaling is a consequence of the absence of a characteristic time scale for the long-time model convergence: it turns out that the relevant scaling exponents are very small: empirically the GCM convergence is “ultra slow” (Lovejoy et al., 2013) (section 3.4). Most earlier studies focused on the implications of the long – range statistical dependencies implicit in the scaling statistics. Unfortunately, due to this rather technical focus, the broader implications of the scaling have not been widely appreciated.

More recently, using scaling fluctuation analysis, behavior has been put into the general theoretical framework of GCM climate modeling (Lovejoy et al., 2013). From the scaling point of view, it appears that the climate arises as a consequence of slow internal climate processes combined with external forcings (especially volcanic and solar - and in the recent period - anthropogenic forcings). From the point of view of the GCMs, the low frequency (multicentennial) variability arises exclusively as a response to external forcings, although potentially - with the addition of (known or currently unknown) slow processes such as land-ice or biogeochemical processes - new internal sources of low frequency variability could be included. Ignoring the recent (industrial) period, and confining ourselves to the last millennium, the key question for GCM models is whether or not they can reproduce the climate regime where the decline of the “macroweather” fluctuations ($H < 0$) is arrested and the increasing $H > 0$ climate regime fluctuations begin. In a recent publication (Lovejoy et al., 2013), four GCMs simulating the last millennium were statistically analyzed and it was found that their low frequency variability (especially below $(100 \text{ yrs})^{-1}$) was somewhat weak, and this was linked to both the weakness of the solar forcings (when using sunspot-based solar reconstructions with $H > 0$), and – for strong volcanic forcings - with the statistical type of the forcing ($H < 0$, Lovejoy and Schertzer, 2012a; Bothe et al., 2013a,b; Zanchettin et al., 2013; see also Zanchettin et al., 2010, for the dynamics on centennial time scales).

1.4 This paper

The weakness of the responses to solar and volcanic forcings at multicentennial scales raises question a linearity question: is the response of the combined (solar plus volcanic) forcing roughly the sum of the individual responses? Additivity is often implicitly assumed when climate forcings are reduced to their equivalent radiative forcings and Mann et al., (2005) already pointed out that – at least - in the Zebiac-Cane (ZC) model discussed below that they are not additive. Here we more precisely analyze this question and quantify the degree of sub-additivity as a function of temporal scale (section 3.4). A related linear/nonlinear issue pointed out by Clement et al., (1996), is that due to the nonlinear model response, there is a high sensitivity to a small forcing and a low sensitivity to a large forcing. Systems in which strong and weak events have different statistical behaviors display stronger or weaker “clustering” and are often termed “intermittent” (from turbulence). When they are also scaling, the weak and strong events are characterized by different scaling exponents that quantify how the respective clustering changes with scale. In section 4, we investigate this quantitatively and confirm that it is particularly strong for volcanic forcing, and that for the ZC

Διαγράφηκε: Using benthic paleotemperature proxies, this scaling picture was recently extended to “macroclimate” ($H < 0$)

Διαγράφηκε: $H > 0$

Διαγράφηκε: for a discussion and wide scale range composite analyses) using both spectra and fluctuation analysis.

Διαγράφηκε: τ_c

Διαγράφηκε: . The Holocene Greenland paleotemperatures show $\tau_c \approx 2000$ yrs whereas pre-Holocene Greenland values are ten times smaller. However, there is other (... [13])

Διαγράφηκε: (...) (... [14])

Διαγράφηκε: [

Αλλαγή κωδικού πεδίου

Διαγράφηκε:]...[(... [15])

Αλλαγή κωδικού πεδίου

Διαγράφηκε:]...[(... [16])

Αλλαγή κωδικού πεδίου

Διαγράφηκε:]...[(... [17])

Αλλαγή κωδικού πεδίου

Διαγράφηκε:]...[(... [18])

Αλλαγή κωδικού πεδίου

Διαγράφηκε:]

Διαγράφηκε: (...] (... [19])

Διαγράφηκε: ... $H < 0$ (... [20])

Διαγράφηκε: (...] (... [21])

Διαγράφηκε: $H > 0$ (...] (... [22])

Διαγράφηκε: [

Αλλαγή κωδικού πεδίου

Διαγράφηκε:]...[(... [23])

Αλλαγή κωδικού πεδίου

Διαγράφηκε:]...; (... [24])

Αλλαγή κωδικού πεδίου

Διαγράφηκε:]... (... [25])

Αλλαγή κωδικού πεδίου

Διαγράφηκε:]

Διαγράφηκε: (...] (... [26])

Αλλαγή κωδικού πεδίου

Διαγράφηκε:]

model the response (including that of a GCM), is much less intermittent, implying that the model strongly (and nonlinearly) smooths the forcing.

In this paper, we establish analysis methodologies that can address these issues and apply them to model outputs that cover the the required range of time scales: Last Millenium model outputs. Unfortunately - although we consider the NASA GISS E2-R Last Millenium simulations, there seem to be no full Last Millenium GCM simulations that have the entire suite of volcanic only, solar only and solar plus volcanic forcings and responses, therefore we have use the simplified Zebiak-Cane model outputs published by Mann et al., (2005).

Although the Zebiak –Cane model lacks several important mechanisms- notably for our purposes deep ocean dynamics - there are clearly sources of low frequency variability present in the model. For example, Goswami and Shukla, (1991) using 360 year control runs found multidecadal and multicentennial nonlinear variability due to the feedbacks between SST anomalies, low level convergence and atmospheric heating. In addition, in justifying his Millenium ZC simulations, (Mann et al., 2005) specifically cited model centennial scale variability as a motivating factor.

2. Data and analysis

2.1 Discussion

During the pre-industrial part of the last millennium, the atmospheric composition was roughly constant, and the earth's orbital parameters varied by only a small amount. The main forcings used in GCM climate models over this period are thus solar and volcanic (in the GISS-E2-R simulations discussed below, reconstructed land use changes are also simulated but the corresponding forcings are comparatively weak and will not be discussed further). In particular, the importance of volcanic forcings was demonstrated by Minnis et al., (1993) who investigated the volcanic radiative forcing caused by the 1991 eruption of Mount Pinatubo, and found that volcanic aerosols produced a strong cooling effect. Later, Shindell et al., (2003) used a stratosphere-resolving general circulation model to examine the effect of the volcanic aerosols and solar irradiance variability on pre-industrial climate change. They found that the best agreement with historical and proxy data was obtained using both forcings. However, solar and volcanic forcings induce different responses because the stratospheric and surface influences in the solar case reinforce one another but in the volcanic case they are opposed. In addition, there are important differences in solar and volcanic temporal variabilities (including seasonality) that statistically link volcanic eruptions with the onset of ENSO events (Mann et al., 2005). Decreased solar irradiance cools the surface and stratosphere (Kondratyev and Varotsos, 1995). In contrast, volcanic eruptions cool the surface, but aerosol heating warms the sunlit lower stratosphere (Shindell et al., 2003; Miller et al., 2012). This leads to an increased meridional gradient in the lower stratosphere, but a reduced gradient in the tropopause region (Chandra et al., 1996; Varotsos et al., 2004).

Vyushin et al., (2004) suggested that volcanic forcings improve the low frequency variability scaling performance of atmosphere-ocean models compared to all other forcings (see however the comment by Blender and Fraedrich, (2004), which also discusses earlier papers on the field e.g. Fraedrich and Blender, (2003); Blender and Fraedrich, (2004). Weber, (2005) used a set of simulations with a climate model, driven by reconstructed forcings in order to study the Northern Hemisphere temperature response to volcanic and solar forcing, during 1000-1850. It was concluded that the response to solar forcing equilibrates at interdecadal timescales, while the response to volcanic forcing never equilibrates due to the fact that the time

Διαγράφηκε: [

Αλλαγή κωδικού πεδίου

Διαγράφηκε:]

Διαγράφηκε: [

Αλλαγή κωδικού πεδίου

Διαγράφηκε:]

Διαγράφηκε:

Διαγράφηκε: ¶

Διαγράφηκε: There have been several studies of the low frequency control run responses of GCMs ; ; ; finding that they are scaling down to their lowest frequencies (by "scaling" we mean a power law change in the statistics when the space and/or time scales are changed, for example, power law spectra). This scaling is a consequence of the abs (... [27]

Αλλαγή κωδικού πεδίου

Διαγράφηκε:). When (... [28]

Διαγράφηκε: [

Αλλαγή κωδικού πεδίου

Διαγράφηκε:]

Διαγράφηκε: [

Αλλαγή κωδικού πεδίου

Διαγράφηκε:]

Αλλαγή κωδικού πεδίου

Διαγράφηκε: [

Αλλαγή κωδικού πεδίου

Διαγράφηκε:]

Διαγράφηκε: [

Αλλαγή κωδικού πεδίου

Διαγράφηκε: [

Αλλαγή κωδικού πεδίου

Διαγράφηκε:]

Διαγράφηκε: .

Διαγράφηκε: [

Αλλαγή κωδικού πεδίου

Διαγράφηκε:]

Διαγράφηκε: [

Αλλαγή κωδικού πεδίου

Διαγράφηκε:]

Αλλαγή κωδικού πεδίου

interval between volcanic eruptions is typically shorter than the dissipation time scale of the climate system (in fact they are scaling so that eruptions occur over all observed time scales, see below).

At the same time, Mann et al. (2005) investigated the response of El Niño to natural radiative forcing changes during 1000-1999, by employing the Zebiak–Cane model for the coupled ocean–atmosphere system in the tropical Pacific. They found that the composite feedback of the volcanic and solar radiative forcing to past changes, reproduces the fluctuations in the variability of the historic El Niño records.

Finally, as discussed below Lovejoy and Schertzer, (2012a) analysed the time scale dependence of several solar reconstructions, Lean. (2000); Wang et al., (2005); Krivova et al., (2007); Steinhilber et al., (2009); Shapiro et al., (2011) and the two main volcanic reconstructions, Crowley, (2000) and Gao et al., (2008), (referred to as “Crowley” and “Gao” in the following). The solar forcings were found to be qualitatively quite different depending on whether the reconstructions were based on sunspots or ^{10}Be isotopes from ice cores with the former increasing with time scale, and the latter decreasing with time scale. This quantitative and qualitative difference brings into question the reliability of the solar reconstructions. By comparison, the two volcanic reconstructions were both statistically similar in type; they were very strong at annual and sometimes multiannual scales but they quickly decrease with time scale ($H < 0$) explaining why they are weak at centennial and millennial scales. We re-examine these findings below.

2.2 The climate simulation of Mann et al. (2005) using the Zebiak-Cane model

Mann et al., (2005) used the Zebiak–Cane model of the tropical Pacific coupled ocean – atmosphere system (Zebiak and Cane, 1987) to produce a 100-realization ensemble for solar forcing only, volcanic forcing only and combined forcings over the last millennium. Figure 1a shows the forcings and mean responses of the model which were obtained from: ftp://ftp.ncdc.noaa.gov/pub/data/paleo/climate_forcing/mann2005/mann2005.txt. No anthropogenic effects were included. Mann et al. [2005] modeled the region between $\pm 30^\circ$ of latitude - by scaling the Crowley volcanic forcing reconstruction with a geometric factor 1.57 to take the limited range of latitudes into account. Figure 1b shows the corresponding GISS-E2-R simulation responses for three different forcings as discussed in Schmidt et al., (2013) and Lovejoy et al., (2013). Although these were averaged over the northern hemisphere land only (a somewhat different geography than the ZC simulations), one can see that the low frequencies seem similar even if the high frequencies are somewhat different. We quantify this below.

3. Methods

3.1 Comparing simulations with observations as functions of scale

The ultimate goal of weather and climate modelling (including forecasting) is to make simulations $T_{sim}(t)$ as close as possible to observations $T_{obs}(t)$. Ignoring measurement errors and simplifying the discussion by only considering a single spatial location (i.e. a single time series), the goal is to achieve simulations with $T_{sim}(t) = T_{obs}(t)$. However, this is not only very ambitious for the simulations, even when considering the observations, $T_{obs}(t)$ is often difficult to evaluate if only because data are often sparse or inadequate in various ways. However, a necessary condition for $T_{sim}(t) = T_{obs}(t)$ is the weaker statistical equality: $T_{sim}(t) \stackrel{d}{=} T_{obs}(t)$ where

Διαγράφηκε:]

Διαγράφηκε: [

Διαγράφηκε:]...:... [... [29]

Αλλαγή κωδικού πεδίου

Διαγράφηκε:]... [... [30]

Διαγράφηκε:]... [... [31]

Διαγράφηκε:]... [... [32]

Αλλαγή κωδικού πεδίου

Διαγράφηκε:]...:... [... [33]

Αλλαγή κωδικού πεδίου

Αλλαγή κωδικού πεδίου

Αλλαγή κωδικού πεδίου

Αλλαγή κωδικού πεδίου

Διαγράφηκε:]

Διαγράφηκε: [

Αλλαγή κωδικού πεδίου

Διαγράφηκε:]... Error! Objects cannot be created from editing field codes... Error! Objects cannot be created from editing field codes. [... [34]

Αλλαγή κωδικού πεδίου

Διαγράφηκε: ... (μ [... [35]

Διαγράφηκε:]... [... [36]

Διαγράφηκε:]...:... [... [37]

Αλλαγή κωδικού πεδίου

Διαγράφηκε:]

Διαγράφηκε: [

Αλλαγή κωδικού πεδίου

Διαγράφηκε:]... [... [38]

Αλλαγή κωδικού πεδίου

Διαγράφηκε:]

Διαγράφηκε: $T_{sim}(t)$... [... [39]

Διαγράφηκε: with.

Διαγράφηκε: $T_{sim}(t) = T_{obs}(t)$... [... [40]

Διαγράφηκε: for

Διαγράφηκε: $T_{sim}(t) = T_{obs}(t)$... [... [41]

$T_{sim}(t) \stackrel{d}{=} T_{obs}(t)$

171 “ $\stackrel{d}{=}$ ” means equal in probability distributions (we can say that $\stackrel{d}{a=b}$ if $\Pr(a>s)=\Pr(b>s)$ where “Pr” indicates “probability”).

172 Although $T_{sim}(t) \stackrel{d}{=} T_{obs}(t)$ is only a necessary (but not sufficient) condition for $T_{sim}(t) = T_{obs}(t)$, it is much easier to empirically verify.

173 Starting in the 1990s, with the advent of ensemble forecasting systems, the Rank Histogram (RH) method was proposed
 174 (Anderson, 1996) as a simple nonparametric test of $T_{sim}(t) \stackrel{d}{=} T_{obs}(t)$, and this has led to a large literature, including recently Bothe et
 175 al., (2013a, b). From our perspective there are two limitations of the RH method. First, it is non-parametric so that its statistical
 176 power is low. More importantly, it essentially tests the equation $T_{sim}(t) \stackrel{d}{=} T_{obs}(t)$ at a single unique time scale/resolution. This is
 177 troublesome since the statistics of both $T_{sim}(t)$ and $T_{obs}(t)$ series will depend on their space-time resolutions; recall that
 178 averaging in space alters the temporal statistics, e.g. $5^{\circ} \times 5^{\circ}$ data are not only spatially, but also are effectively temporally
 179 smoothed with respect to $1^{\circ} \times 1^{\circ}$ data. This means that even if $T_{sim}(t)$ and $T_{obs}(t)$ have nominally the same temporal resolutions
 180 they may easily have different high frequency variability. Possibly more importantly - as claimed in Lovejoy et al., (2013), and
 181 below - the main difference between $T_{sim}(t)$ and $T_{obs}(t)$ may be that the latter has more low frequency variability than the
 182 former, and this will not be captured by the RH technique which operates only at the highest frequency available. This problem
 183 is indirectly acknowledged, see for example the discussion of correlations in Marzban et al., (2011). The potential significance of
 184 the low frequencies becomes obvious when $H > 0$ for the low frequency range. In this case – since the series tends to “wander”,
 185 small differences in the low frequencies may translate into very large differences in RH, and this even if the high frequencies are
 186 relatively accurate.

187 A straightforward solution is to use the same basic idea – i.e. to change the sense of equality from deterministic to
 188 probabilistic (“=” to “ $\stackrel{d}{=}$ ”) – but to compare the statistics systematically over a range of time scales. The simplest way is to
 189 check the equality $\Delta T_{sim}(\Delta t) \stackrel{d}{=} \Delta T_{obs}(\Delta t)$ where ΔT is the fluctuation of the temperature over a time period Δt (see the discussion
 190 in Lovejoy and Schertzer, (2013) box 11.1). In general, knowledge of the probabilities is equivalent to knowledge of (all) the
 191 statistical moments (including the non-integer ones), and for technical reasons it turns out to be easier to check
 192 $\Delta T_{sim}(\Delta t) \stackrel{d}{=} \Delta T_{obs}(\Delta t)$ by considering the statistical moments.

193 3.2 Scaling Fluctuation Analysis

194 In order to isolate the variability as a function of time scale Δt , we estimated the fluctuations $\Delta F(\Delta t)$ (forcings, W/m^2),
 195 $\Delta T(\Delta t)$ (responses, K). Although it is traditional (and often adequate) to define fluctuations by absolute differences
 196 $\Delta T(\Delta t) = |T(t + \Delta t) - T(t)|$, for our purposes this is not sufficient. Instead we should use the absolute difference of the means from t to
 197 $t + \Delta t / 2$ and from $t + \Delta t / 2$ to $t + \Delta t$. Technically, the latter corresponds to defining fluctuations using Haar wavelets rather than
 198 “poor man’s” wavelets (differences). In a scaling regime, the fluctuations vary with the time lag in a power law manner:

$$199 \quad \Delta T = \varphi \Delta t^H \quad (1)$$

Διαγράφηκε: $\stackrel{d}{=} \dots \stackrel{d}{=} b \dots$

$\Pr(a > s) = \Pr(b > s) \dots T_{sim}(t) \stackrel{d}{=} \dots$ [42]

Διαγράφηκε: τ

Διαγράφηκε: $T_{sim}(t) = T_{obs}(t)$

Διαγράφηκε: [

Διαγράφηκε: [

Αλλαγή κωδικού πεδίου

Διαγράφηκε:]

Διαγράφηκε: $T_{sim}(t) \stackrel{d}{=} T_{obs}(t)$

Αλλαγή κωδικού πεδίου

Διαγράφηκε: ;

Διαγράφηκε:]

Διαγράφηκε: equation

Διαγράφηκε: $T_{sim}(t) \stackrel{d}{=} T_{obs}(t) \dots$

$T_{sim}(t)$ [43]

Διαγράφηκε: a

Διαγράφηκε: $T_{obs}(t) \dots T_{sim}(t) \dots$

$T_{obs}(t)$ [44]

Διαγράφηκε: [

Αλλαγή κωδικού πεδίου

Διαγράφηκε:]

Διαγράφηκε: $T_{sim}(t) \dots$ [45]

Διαγράφηκε: [

Αλλαγή κωδικού πεδίου

Διαγράφηκε:]

Διαγράφηκε: $H > 0$

Διαγράφηκε: $\stackrel{d}{=} \dots$

$\Delta T_{sim}(\Delta t) \stackrel{d}{=} \Delta T_{obs}(\Delta t)$ [46]

Διαγράφηκε: [

Αλλαγή κωδικού πεδίου

Διαγράφηκε:]

Διαγράφηκε: $\Delta T_{sim}(\Delta t) \stackrel{d}{=} \Delta T_{obs}(\Delta t)$

Διαγράφηκε: 1

Διαγράφηκε: $\Delta F(\Delta t) \dots$ [47]

Διαγράφηκε: $\Delta T = \varphi \Delta t^H$

Μορφοποιήθηκε [48]

Διαγράφηκε: 1

where ϕ is a controlling dynamical variable (e.g. a dynamical flux) whose mean $\langle \phi \rangle$ is independent of the lag Δt (i.e. independent of the time scale). This means that the behaviour of the mean fluctuation is $\langle \Delta T \rangle \approx \Delta t^H$ so that when $H > 0$, on average fluctuations tend to grow with scale whereas when $H < 0$, they tend to decrease. Note that the symbol “ H ” is in honour of Harold Edwin Hurst (Hurst, 1951). Although in the case of quasi-Gaussian statistics, it is equal to his eponymous exponent, the H used here is valid in the more general multifractal case and is generally different.

Fluctuations defined as differences are adequate for fluctuations increasing with scale ($H > 0$). When $H > 0$, the rate at which average differences increase with time lag Δt directly reflects the increasing importance of low frequencies with respect to high frequencies. However, in physical systems the differences tend to increase even when $H < 0$. This is because correlations $\langle T(t + \Delta t)T(t) \rangle$ tend to decrease with the time lag Δt and this directly implies that the mean square differences $\langle (\Delta T(\Delta t))^2 \rangle$ increase (mathematically, for a stationary process: $\langle \Delta T(\Delta t)^2 \rangle = \langle (T(t + \Delta t) - T(t))^2 \rangle = 2(\langle T^2 \rangle - \langle T(t + \Delta t)T(t) \rangle)$). This means that when $H < 0$, differences cannot correctly characterize the fluctuations. For $H < 0$ the high-frequency details dominate the differences and prevent these differences to decrease with increasing scale Δt .

The Haar fluctuation which is useful for $-1 < H < 1$ is particularly easy to understand since with proper “calibration” in regions where $H > 0$, its value can be made to be very close to the difference fluctuation, while in regions where $H < 0$, it can be made close to another simple to interpret “anomaly fluctuation”. The latter is simply the temporal average of the series over a duration Δt of the series with its overall mean removed (in Lovejoy and Schertzer, 2012b this was termed a “tendency” fluctuation which is a less intuitive term). In this case, the decrease of the Haar fluctuations for increasing lag Δt characterizes how effectively averaging a (mean zero) process (the anomaly) over longer time scales reduces its variability. Here, the calibration is affected by multiplying the raw Haar fluctuation by a factor of 2 which brings the values of the Haar fluctuations very close to both the corresponding difference and anomaly fluctuations (over time scales with $H > 0$, $H < 0$ respectively). This means that in regions where $H > 0$, to good accuracy, the Haar fluctuations can be treated as differences whereas in regions where $H < 0$ they can be treated as anomalies. While other techniques such as Detrended Fluctuation Analysis (Peng et al., 1994) perform just as well for determining exponents, they have the disadvantage that their fluctuations are not at all easy to interpret (they are the standard deviations of the residues of polynomial regressions on the running sum of the original series).

Once estimated, the variation of the fluctuations with time scale can be quantified by using their statistics; the q^{th} order structure function $s_q(\Delta t)$ is particularly convenient:

$$s_q(\Delta t) = \langle \Delta T(\Delta t)^q \rangle \quad (2)$$

where “ $\langle \rangle$ ” indicates ensemble averaging (here, we average over all disjoint intervals of length Δt). Note that although q can in principle be any value, here we restrict to $q > 0$ since divergences may occur – indeed for multifractals, are expected - for $q < 0$). In a scaling regime, $s_q(\Delta t)$ is a power law:

$$s_q(\Delta t) = \langle \Delta T(\Delta t)^q \rangle \propto \Delta t^{\xi(q)}; \xi(q) = qH - K(q) \quad (3)$$

Διαγράφηκε: $\langle \phi \rangle \dots \Delta t \dots$
 $\langle \Delta T \rangle \approx \Delta t^H \dots H > 0 \dots H < 0 \dots$ [49]

Διαγράφηκε: [...] [50]

Διαγράφηκε: $(H > 0) \dots H > 0$
 $\Delta t \dots H < 0$ [51]

Διαγράφηκε: $\langle T(t + \Delta t)T(t) \rangle \dots$

Διαγράφηκε: $\langle T(t + \Delta t)T(t) \rangle \dots$
 $\langle \Delta T(\Delta t)^2 \rangle = \langle (T(t + \Delta t) - T(t))^2 \rangle = 2(\langle T^2 \rangle - \langle T(t + \Delta t)T(t) \rangle)$
 $H < 0 \dots H < 0 \dots \Delta t$ [52]

Διαγράφηκε: Technically, this reflects the fact that the fluctuations at scale Δt are no longer determined by frequencies near $1/\Delta t$ but rather by irrelevant low frequency details of the empirical sample.

Διαγράφηκε: $H > 0 \dots H < 0 \dots$
 Δt [53]

Διαγράφηκε: [

Αλλαγή κωδικού πεδίου

Διαγράφηκε: c... [54]

Διαγράφηκε: $\Delta t \dots H > 0 \dots H < 0$
 0 [55]

Διαγράφηκε: ,

Διαγράφηκε: $H > 0 \dots$ [56]

Διαγράφηκε: ,

Διαγράφηκε: [

Αλλαγή κωδικού πεδίου

Διαγράφηκε:]

Διαγράφηκε: $s_q(\Delta t)$

Διαγράφηκε: $s_q(\Delta t) = \langle \Delta T(\Delta t)^q \rangle$

Μορφοποιήθηκε:
 Γραμματοσειρά:
 (Προεπιλεγμένη) Times
 New Roman, 10 pt, Χρώμα
 γραμματοσειράς: Μαύρο,
 Χωρίς ορθογραφικό ή
 γραμματικό έλεγχο

Διαγράφηκε: 2

Διαγράφηκε: $\langle \dots \Delta t \dots s_q(\Delta t) \dots$ [57]

Διαγράφηκε: $s_q(\Delta t) = \langle \Delta T(\Delta t)^q \rangle$

231 where the exponent $\xi(q)$ has a linear part qH and a generally nonlinear and convex part $K(q)$ with $K(1)=0$. $K(q)$
 232 characterizes the strong non Gaussian, multifractal variability; the “intermittency”. Gaussian processes have $K(q)=0$. The root-
 233 mean-square (RMS) variation $S_2(\Delta)^{1/2}$ (denoted simply $S(\Delta)$ below) has the exponent $\xi(2)/2 = H - K(2)/2$. It is only when
 234 the intermittency is small ($K(q) \approx 0$) that we have $\xi(2)/2 \approx H = \xi(1)$. Note that since the spectrum is a second order statistic, we have
 235 the useful relationship for the exponent β of the power law spectra: $\beta = 1 + \xi(2) = 1 + 2H - K(2)$ (this is a corollary of the Wiener-
 236 Khintchin theorem). Again, only when $K(2)$ is small do we have the commonly used relation $\beta \approx 1 + 2H$; in this case, $H > 0$,
 237 $H < 0$ corresponds to $\beta > 1$, $\beta < 1$ respectively. To get an idea of the implications of the nonlinear $K(q)$, note that a high q value
 238 characterizes the scaling of the strong events whereas a low q characterizes the scaling of the weak events (q is not restricted to
 239 integer. The scalings are different whenever the strong and weak events cluster to different degrees, the clustering in turn is
 240 precisely determined by another exponent - the codimension - which is itself uniquely determined by $K(q)$. We return to the
 241 phenomenon of “intermittency”, in section 4, it is particularly pronounced in the case of volcanic forcings.

242 Figure 2a shows the result of estimating the Haar fluctuations for the solar and volcanic forcings. The solar reconstruction
 243 that was used is a hybrid obtained by “splicing” the annual resolution sunspot based reconstruction (Fig. 2b, top; back to 1610,
 244 although only the more recent part was used by Mann et al. (2005) with a ^{10}Be based reconstruction (Fig. 2b, bottom) at much
 245 lower resolution (≈ 40 -50 yrs). In Fig. 2a, the two rightmost curves are for two different ^{10}Be reconstructions; at any given time
 246 scale, their amplitudes differ by nearly a factor of 10 yet they both have Haar fluctuations that diminish with scale ($H \approx -0.3$).
 247 Figure 2b (top) clearly shows the qualitative difference with “wandering” ($H > 0$, sunspot based) and Fig. 2b (bottom), the
 248 cancelling ($H < 0$, ^{10}Be based) solar reconstructions (Lovejoy and Schertzer, 2012a). In the “spliced” reconstruction used here,
 249 the early ^{10}Be part (1000-1610) at low resolution was interpolated to annual resolution; the interpolation was close to linear so
 250 that we find $H \approx 1$ over the scale range 1-50 yrs, with the $H < 0$ part barely visible over the range 100-600 years (roughly the
 251 length of the ^{10}Be part of the reconstruction).

252 The reference lines in Fig. 2a have slopes -0.4, -0.3, 0.4 showing that both solar and volcanic forcings are fairly accurately
 253 scaling (although because of the “splicing” for the solar, only up until ≈ 200 -300 yrs) but with exactly opposite behaviours:
 254 whereas the solar fluctuations increase with time scale, the volcanic fluctuations decrease with scale. For time scales beyond
 255 200-300 yrs, the solar forcing is stronger than the volcanic forcing (they “cross” at roughly 0.3 W/m^2).

256 3.3 Linearity and nonlinearity

257 There is no question that - at least in the usual deterministic sense - the atmosphere is turbulent and nonlinear. Indeed, the ratio of
 258 the nonlinear to the linear terms in the dynamical equations - the Reynolds number - is typically about 10^{12} . Due to the smaller
 259 range of scales, in the numerical models it is much lower, but it is still $\approx 10^3$ to 10^4 . Indeed it turns out that the variability builds
 260 up scale by scale from large to small scales so that - since the dissipation scale is about 10^{-3} m - the resulting (millimetre scale)
 261 variability can be enormous; the statistics of this buildup are quite accurately modelled by multifractal cascades (see the review
 262 Lovejoy and Schertzer, 2013, especially ch. 4 for cascade analyses of data and model outputs). The cascade based Fractionally

Διαγράφηκε: $\xi(q) \dots qH$
 $K(q) \dots K(1)=0 \dots K(q) \dots K(q)=0$
 $S_2(\Delta)^{1/2} \dots S(\Delta) \dots$
 $\xi(2)/2 = H - K(2)/2 \dots K(q) \approx 0 \dots$
 $\xi(2)/2 \approx H = \xi(1) \dots$
 $\beta = 1 + \xi(2) = 1 + 2H - K$
 $K(2) \dots \beta = 1 + 2H \dots H > 0 \dots \frac{H < 0}{\dots [58]}$

Διαγράφηκε:

Διαγράφηκε: $\square > 1 \dots [59]$

Διαγράφηκε: to ,

Διαγράφηκε: $K(q) \dots [60]$

Διαγράφηκε: f...ure... [61]

Διαγράφηκε: f

Διαγράφηκε: ure...e [62]

Διαγράφηκε: f

Διαγράφηκε: ure...H [63]

Διαγράφηκε: left

Διαγράφηκε: $H > 0 \dots [64]$

Διαγράφηκε: right

Διαγράφηκε: $H < 0$

Διαγράφηκε: [

Αλλαγή κωδικού πεδίου

Διαγράφηκε:]

Διαγράφηκε: $H=1 \dots \text{ea} \dots H <$

Διαγράφηκε: 0 [65]

Διαγράφηκε:

Διαγράφηκε: f

Διαγράφηκε: ure...e [66]

Διαγράφηκε: ¶

Διαγράφηκε: 3.2 The

Uncertainty in $S(\Delta)$ ¶

Let us briefly discuss the

uncertainty with which $S(\Delta)$

is estimated, i.e. the

deviations of the estimated

$S(\Delta)$ from its true value.

There are several sources of

uncertainty to consider. The

most problematic are [67]

Διαγράφηκε: Let us [68]

Διαγράφηκε: 3

Διαγράφηκε: [

Αλλαγή κωδικού πεδίου

Διαγράφηκε:]

263 Integrated Flux model (FIF, Schertzer and Lovejoy, 1987) is a nonlinear stochastic model of the weather scale dynamics,
264 and can be extended to provide nonlinear stochastic models of the macroweather and climate regimes (Lovejoy and Schertzer,
265 2013, ch. 10).

266 However, ever since Hasselmann, (1976), it has been proposed that sufficiently space-time averaged variables may
267 respond linearly to sufficiently space-time averaged forcings. In the resulting (low frequency) phenomenological models, the
268 nonlinear deterministic (high frequency) dynamics act as a source of random perturbations; the resulting stochastic model is
269 usually taken as being linear. Such models are only justified if there is a physical scale separation between the high frequency
270 and low frequency processes. The existence of a relevant break (at 2- 10 day scales) has been known since Panofsky and Van der
271 Hoven, (1955) and was variously theorized as the “scale of migratory pressure systems of synoptic weather map scale” (Van der
272 Hoven, 1957) and later as the “synoptic maximum” (Kolesnikov and Monin, 1965). From the point of view of Hasselman-type
273 linear stochastic modelling (now often referred to as “Linear Inverse Modelling (LIM)”, e.g., Penland and Sardeshmuhk, (1995);
274 Newman et al., (2003); Sardeshmukh and Sura, (2009)), the system is regarded as a multivariate Ornstein-Uhlenbeck (OU)
275 process. At high frequencies, an OU process is essentially the integral of a white noise (with spectrum $\omega^{-\beta_h}$ with $\beta_h = 2$), whereas
276 at low frequencies it is a white noise, (i.e. $\omega^{-\beta_l}$ with $\beta_l = 0$). In the LIM models, these regimes correspond to the weather and
277 macroweather, respectively. Recently Newman, (2013) has shown predictive skill for global temperature hindcasts is somewhat
278 superior to GCM’s for 1-2 year horizons.

279 In the more general scaling picture going back to Lovejoy and Schertzer, (1986), the transition corresponds to the lifetime
280 of planetary structures. This interpretation was quantitatively justified in (Lovejoy and Schertzer, 2010) by using the turbulent
281 energy rate density. The low and high frequency regimes were scaling and had spectra significantly different than those of OU
282 processes (notably with $0.2 < \beta_l < 0.8$) with the two regimes now being referred to as “weather” and “macroweather” (Lovejoy and
283 Schertzer, 2013). Indeed, the main difference with respect to the classical LIM is at low frequencies. Although the difference in
284 β_l may not seem so important, the LIM value $\beta_l = 0$, (white noise) has no low frequency predictability whereas the actual
285 values $0.2 < \beta_l < 0.8$ (depending mostly on the land or ocean location) corresponds to potentially huge predictability (the latter can
286 diverge as β_l approaches 1). A new “ScaLIng Macroweather Model” (SLIMM) has been proposed as a set of fractional order
287 (but still linear) stochastic differential equations with predictive skill for global mean temperatures out to at least 10 years
288 (Lovejoy et al., 2015; Lovejoy, 2015b). However, irrespective of the exact statistical nature of the weather and macroweather
289 regimes, a linear stochastic model may still be a valid approximation over significant ranges.

290 These linear stochastic models (whether LIM or SLIMM) explicitly exploit the weather/macroweather transition and may
291 have some skill up to macroweather scales perhaps as large as decades. However, at longer time scales, another class of
292 phenomenological model is often used, wherein the dynamics are determined by radiative energy balances. Energy balance
293 models focus on slower (true) climate scale processes such as sea ice – albedo feedbacks and are generally quite nonlinear, being
294 associated with nonlinear features such as tipping points and bifurcations (Budyko, 1969). These models are typically zero or one
295 dimensional in space (i.e. they are averaged over the whole earth or over latitude bands) and may be deterministic or stochastic
296 (see (Nicolis, 1988) for an early comparison of the two approaches). See Dijkstra, (2013) for a survey of the classical
297 deterministic dynamical systems approach as well as the more recent stochastic “random dynamical systems” approach, (see also
298 Ragone, et al., 2014).

- Διαγράφηκε: [...]... [69]
- Αλλαγή κωδικού π[...] [70]
- Διαγράφηκε: []
- Διαγράφηκε: []
- Αλλαγή κωδικού π[...] [71]
- Διαγράφηκε: [...]... [72]
- Αλλαγή κωδικού π[...] [73]
- Διαγράφηκε: [...]... [74]
- Αλλαγή κωδικού π[...] [75]
- Διαγράφηκε: [...]... [76]
- Αλλαγή κωδικού π[...] [77]
- Διαγράφηκε: [...]... [78]
- Αλλαγή κωδικού π[...] [79]
- Διαγράφηκε: [...]... [80]
- Διαγράφηκε: [...]... [81]
- Αλλαγή κωδικού π[...] [82]
- Διαγράφηκε: []
- Αλλαγή κωδικού π[...] [83]
- Διαγράφηκε: $\omega^{-\beta}$
- Διαγράφηκε: with $\beta_h = 2$
- Διαγράφηκε: $\omega^{-\beta} \dots \beta^{-f}$ [84]
- Διαγράφηκε: []
- Αλλαγή κωδικού π[...] [85]
- Διαγράφηκε: []
- Διαγράφηκε: []
- Αλλαγή κωδικού π[...] [86]
- Διαγράφηκε: [...]... [87]
- Αλλαγή κωδικού π[...] [88]
- Διαγράφηκε: []
- Διαγράφηκε: β_l
- Διαγράφηκε: []
- Αλλαγή κωδικού π[...] [89]
- Διαγράφηκε: []
- Διαγράφηκε: $\beta_l \dots \beta^{-f} \beta$ [90]
- Διαγράφηκε: Scaling [91]
- Διαγράφηκε: []
- Αλλαγή κωδικού π[...] [92]
- Διαγράφηκε: [...]... [93]
- Αλλαγή κωδικού π[...] [94]
- Διαγράφηκε: []
- Διαγράφηκε: ()
- Διαγράφηκε: [...]... [95]
- Διαγράφηκε: []
- Αλλαγή κωδικού π[...] [96]
- Διαγράφηκε: [...]... [97]

299 Although energy balance models are almost always nonlinear, there have been several suggestions that linear
 300 energy balance models are in fact valid up to millennial and even multimillennial scales. Finally, we could mention the existence
 301 of empirical evidence of stochastic linearity between forcings and responses in the macroweather regime. Such evidence comes
 302 for example, from the apparent ability of linear regressions to “remove” the effects of volcanic, solar and anthropogenic forcings
 303 (Lean and Rind, 2008). This has perhaps been quantitatively demonstrated in the case of anthropogenic forcing where use is
 304 made of the globally, annually averaged CO₂ radiative forcings (as a linear surrogate for all anthropogenic forcings). When this
 305 radiative forcing was regressed against similarly averaged temperatures, it gave residues with amplitudes $\pm 0.109\text{K}$ (Lovejoy,
 306 2014a) which is almost exactly the same as GCM estimates of the natural variability (e.g., Laepple et al., (2008)). Notice that in
 307 this case the identification of the global temperature T_{globe} as the sum of a regression determined anthropogenic component (T_{anth})
 308 with residues as natural variability (T_{nat}) is in fact only a confirmation of *stochastic* linearity (i.e. $T_{globe}^d = T_{anth} + T_{nat}$). Since
 309 presumably the actual residues would have been different if there had been no anthropogenic forcing. Indeed, when the residues
 310 were analysed using fluctuation analysis, it was only their statistics that were close to the pre-industrial multiproxy statistics.

311 3.4 Testing linearity: the additivity of the responses

312 We can now test the linearity of the model responses to solar and volcanic forcings. First consider the model responses (Fig. 3a).
 313 Compare the response to the volcanic only forcing (green) curve; with the response from the solar only forcing (black). As
 314 expected from Fig. 2a, the former is stronger than the latter up (until centennial scales) reflecting the stronger volcanic forcing.
 315 At scales $\Delta t \approx 100$ yrs however, we see that the solar only has a stronger response, also as expected from Fig. 2a. Now consider
 316 the response to the combined volcanic and solar forcing (brown). Unsurprisingly, it is very close to the volcanic only until
 317 $\Delta t \approx 100$ yrs; however at longer time scales, the combined response seems to decrease following the volcanic forcing curve; it
 318 seems that at these longer time scales the volcanic and solar forcings have negative feedbacks so that the combined response to
 319 solar plus volcanic forcing is actually less than for pure solar forcing, they are “subadditive”.

320 In order to quantify this we can easily determine the expected solar and volcanic response if the two were combined
 321 additively (linearly). In the latter case, the solar and volcanic fluctuations would not interfere with each other, and since forcings
 322 are statistically independent, the responses would also be statistically independent, the response variances would add.

323 A linear response means that temperature fluctuations due to only solar forcing ($\Delta T_s(\Delta t)$) and only volcanic forcing
 324 ($\Delta T_v(\Delta t)$) would be related to the temperature fluctuations of the response to the combined solar plus volcanic forcings ($\Delta T_{s,v}(\Delta t)$)
 325 as:

$$326 \quad \Delta T_{s,v}(\Delta t) = \Delta T_s(\Delta t) + \Delta T_v(\Delta t) \quad (4)$$

327 This is true regardless of the exact definition of the fluctuation: as long as the fluctuation is defined by a linear operation on the
 328 temperature series any wavelet will do. Therefore, squaring both sides and averaging (“ $\langle \rangle$ ”) and assuming that the fluctuations
 329 in the solar and volcanic forcings are statistically independent of each other (i.e., $\langle \Delta T_s(\Delta t) \Delta T_v(\Delta t) \rangle = 0$), we obtain:

$$330 \quad \langle \Delta T_{s,v}(\Delta t)^2 \rangle = \langle \Delta T_s(\Delta t)^2 \rangle + \langle \Delta T_v(\Delta t)^2 \rangle \quad (5)$$

Διαγράφηκε: .

Διαγράφηκε: ... ; [... [98]

Διαγράφηκε: ¶

Διαγράφηκε: /

Αλλαγή κωδικού πεδίου

Διαγράφηκε:]...[[... [99]

Αλλαγή κωδικού πεδίου

Διαγράφηκε:]...[... [100]

Αλλαγή κωδικού πεδίου

Διαγράφηκε:]...: [... [101]

Διαγράφηκε: $T_{globe}^d = T_{anth} + T_{nat}$

$T_{globe}^d = T_{anth} + T_{nat} \dots \dots \dots$ [... [102]

Διαγράφηκε: ¶

Διαγράφηκε: 4

Διαγράφηκε: f

Διαγράφηκε: ure

Διαγράφηκε: f

Διαγράφηκε: ure... [... [103]

Διαγράφηκε: f

Διαγράφηκε: ure... [... [104]

Διαγράφηκε: $(\Delta T_s(\Delta t)) \dots$

$(\Delta T_s(\Delta t)) \dots \dots \dots \Delta T_{s,v}(\Delta t)$ [... [105]

Διαγράφηκε: $\Delta T_{s,v}(\Delta t) = \Delta T_s(\Delta t) +$

Μορφοποιήθηκε:
 Γραμματοσειρά:
 (Προεπιλεγμένη) Times
 New Roman, 10 pt, Χρώμα
 γραμματοσειράς: Μαύρο,
 Χωρίς ορθογραφικό ή
 γραμματικό έλεγχο

Διαγράφηκε: 4

Διαγράφηκε: $\langle \rangle \dots$

$\langle \Delta T_s(\Delta t) \Delta T_s(\Delta t) \rangle = 0$ [... [106]

Διαγράφηκε: $\langle \Delta T_{s,v}(\Delta t)^2 \rangle$

Μορφοποιήθηκε:
 Γραμματοσειρά:
 (Προεπιλεγμένη) Times
 New Roman, 10 pt, Χρώμα
 γραμματοσειράς: Μαύρο,
 Χωρίς ορθογραφικό ή
 γραμματικό έλεγχο

Διαγράφηκε: 5

331 The implied additive response structure function $s(\Delta t) = \left(\langle \Delta T_s(\Delta t)^2 \rangle + \langle \Delta T_v(\Delta t)^2 \rangle \right)^{1/2}$ is shown in Fig. 3b along with the ratio
 332 of the latter to the actual (nonlinear) solar plus volcanic response (top: $\left(\langle \Delta T_s(\Delta t)^2 \rangle + \langle \Delta T_v(\Delta t)^2 \rangle \right)^{1/2} / \langle \Delta T_{s,v}(\Delta t)^2 \rangle^{1/2}$). It can be seen that
 333 the ratio is fairly close to unity for time scales below about 50 yrs. However beyond 50 yrs there is indeed a strong negative
 334 feedback between the solar and volcanic forcings. This is seen more clearly in Fig. 3c which shows that at $\Delta t \approx 400$ years, that the
 335 negative feedback is strong enough to reduce the theoretical additive fluctuation amplitudes by a factor of ≈ 2.5 (the fall-off at the
 336 largest Δt is probably an artefact of the poor statistics at these scales). It should be noted that the latter holds assuming
 337 independence (pink curve in Fig. 3c) of the solar and volcanic forcing. For comparison, the purple curve in Fig. 3c illustrates the
 338 results obtained when analyzing the series constructed by directly summing the two response series (instead of assuming
 339 statistical independence). It is clearly seen that the basic result still holds but it is a little less strong (a factor of ≈ 2). The reason
 340 for the difference is that the cancellation of the cross terms assumed by statistical independence is only approximately valid on
 341 simple realizations, especially at the lower frequencies where the statistics are worse.

342 In the ZC model, all forcings are input at the surface so that here the subadditivity is due to the differing seasonality,
 343 fluctuation intensities and spatial distributions of the solar and volcanic forcings. In the GISS-E2-R GCM simulations, the
 344 response to the solar forcing is too small to allow us to determine if it involves a similar solar-volcanic negative feedback (Fig. 4).
 345 In GCMs with their vertically stratified atmospheres or the real atmosphere, non additivity is perhaps not surprising given the
 346 difference between the solar and volcanic vertical heating profiles. If such negative feedbacks are substantiated in further
 347 simulations, it would enhance the credibility of the idea that current GCMs are missing critical slow (multi centennial, multi
 348 millennial) climate processes. No matter what the exact explanation, non additivity underlines the limitations of the convenient
 349 reduction of climate forcings to radiative forcing equivalents. It also indicates that at scales longer than about 50 yrs energy
 350 budget models must nonlinearly account for albedo-temperature interactions (i.e. that linear energy budget models are inadequate
 351 at these time scales, and that albedo-temperature interactions must at least be correctly parametrized).

352 Also shown for reference in Fig. 3a are the fluctuations for three multiproxy estimates of annual northern hemisphere
 353 temperatures (1500-1900; pre-industrial, Moberg et al., 2005; Huang, 2004; Ljungqvist, 2010, the analysis was taken from
 354 Lovejoy and Schertzer, 2012c). Although it should be borne in mind that the ZC model region (the Pacific) does not coincide
 355 with the proxy region (the northern hemisphere), the latter is the best model validation available. In addition, since we compare
 356 model and proxy fluctuation statistics as functions of time scale, the fact that the spatial regions are somewhat different is less
 357 important than if we had attempted a direct year by year comparison of model outputs with the multiproxy reconstructions.

358 In Fig. 3a, we see that the responses of the volcanic only and the combined volcanic and solar forcings fairly well
 359 reproduce the RMS multiproxy statistics until ≈ 50 yrs; however at longer time scales, the model fluctuations are substantially
 360 too weak – roughly 0.1 K (corresponding to ± 0.05 K) and constant or falling, whereas at 400 yr scales, the RMS multiproxy
 361 temperature fluctuations are ≈ 0.25 K (± 0.125) and rising. Indeed, in order to account for the ice ages, they must continue to rise
 362 until ≈ 5 K (± 2.5 K) at glacial-interglacial scales of 50 – 100 kyrs, (according to paleodata, this rise continues in a smooth, power
 363 law manner with $H > 0$ until roughly 100 kyrs, see Lovejoy and Schertzer, 1986, Shackleton and Imbrie, 1990 Pelletier, 1998,
 364 Schmitt et al., 1995, Ashkenazy et al., 2003, Huybers and Curry, 2006, and Lovejoy et al., 2013).

365 In Fig. 4, we compare the RMS Haar fluctuations from the ZC model combined (volcanic and solar forcing) response
 366 with those from simulations from the GISS-E2-R GCM with solar only forcing and a control run (no forcings, black; see

331 Διαγράφηκε: $S(\Delta t) = \left(\langle \Delta T_s(\Delta t)^2 \rangle + \langle \Delta T_v(\Delta t)^2 \rangle \right)^{1/2}$

332 Διαγράφηκε: f

333 Διαγράφηκε: ure...
 $\left(\langle \Delta T_s(\Delta t)^2 \rangle + \langle \Delta T_v(\Delta t)^2 \rangle \right)^{1/2} / \langle \Delta T_{s,v}(\Delta t)^2 \rangle^{1/2}$
 ea...ea (... [107])

334 Διαγράφηκε: f

335 Διαγράφηκε: ure... $\Delta t \approx 400$
 $\Delta t \dots ure$ (... [108])

336 Διαγράφηκε: reasons

337 Διαγράφηκε: ure

338 Διαγράφηκε: s

344 Διαγράφηκε: f

345 Διαγράφηκε: ure... (... [109])

351 Διαγράφηκε: parametrised

352 Διαγράφηκε: f

353 Διαγράφηκε: ure

354 Διαγράφηκε: [

355 Διαγράφηκε:]...[(... [110])

356 Αλλαγή κωδικού πεδίου

357 Διαγράφηκε:]...[(... [111])

358 Αλλαγή κωδικού πεδίου

359 Διαγράφηκε:]...[(... [112])

360 Αλλαγή κωδικού πεδίου

361 Αλλαγή κωδικού πεδίου

362 Διαγράφηκε: b...[(... [113])

363 Διαγράφηκε: f

364 Διαγράφηκε: ure... (... [114])

365 Διαγράφηκε: [

366 Αλλαγή κωδικού πεδίου

367 Διαγράφηκε:]

368 Διαγράφηκε: ure

Lovejoy et al., (2013) for details; the GISS-E2-R solar forcing was the same as the spliced series used in the ZC simulations). We see that the three are remarkably close over the entire range; for the GISS model, this indicates that the solar only forcing is so small that the response is nearly the same as for the unforced (control) run. The ZC combined solar and volcanic forcing is clearly much weaker than the pre-industrial multiproxies (dashed blue, same as in Fig. 3a). The reference line with slope -0.2 shows the convergence of the control to the model climate; the shallowness of the slope (-0.2) implies that the convergence is ultra slow. For example, fluctuations from a 10 yr run control run are only reduced by a factor of $(10/3000)^{-0.2} \approx 3$ if the run is extended to 3 kyrs.

Finally, in Fig. 5, we compare the responses to the volcanic forcings for the Zebiak-Cane model and for the GISS-E2-R GCM for two different volcanic reconstructions (Gao et al., 2008), and Crowley, 2000) (the reconstruction used in the ZC simulation). For reference, we again show the combined ZC response and the preindustrial multiproxies. We see that the GISS GCM is much more sensitive to the volcanic forcing than the Zebiak-Cane model; indeed, it is too sensitive at scales $\Delta t \approx 100$, but nevertheless becomes too weak at scales $\Delta t \approx 200$ years. Indeed, since the volcanic forcings continue to decrease with scale, we expect the responses to keep diminishing with scale at larger Δt .

Note that the spatial regions covered by the ZC simulation, the GISS outputs and the multiproxy reconstructions are not the same. For the latter, the reason is that there is no perfectly appropriate (regionally defined) multiproxy series whereas for the GISS outputs, we reproduced the structure function analysis from a published source. Yet, the differences in the regions may not be so important since we are only making statistical comparisons. This is especially true since all the series are for planetary scale temperatures (even if they are not identical global sized regions) and in addition, we are mostly interested in the fifty year (and longer) statistics which may be quite similar.

4. Intermittency: a multifractal trace moment analysis

4.1 The Trace moment analysis technique

In the previous sections we considered the implications of linearity when climate models were forced separately with two different forcings compared with the response to the combined forcing; we showed that the ZC model was subadditive. However, linearity also constrains the relation between the fluctuations in the forcings and the responses. For example at least since the work of Clement et al., (1996), in the context of volcanic eruptions, it has been recognized that the models are typically sensitive to weak forcing events but insensitive to strong ones, i.e. they are nonlinear, and Mann et al., (2005) noticed this in their ZC simulations.

In a scaling regime, both forcings and responses will be characterized by a hierarchy of exponents (i.e. the function $\xi(q)$ in Eq. 3 or equivalently by the exponent H and the function $K(q)$), the differences in the statistics of weak and strong events are reflected in these different exponents; high order moments (large q) are dominated by large fluctuations and conversely for low order moments. The degree of convexity of $K(q)$ quantifies the degree of these nonlinear effects (indeed, how they vary over time scales Δt). Such “intermittent” behaviour was first studied in the context of turbulence (Kolmogorov, 1962; Mandelbrot, 1974).

Διαγράφηκε: ure

Διαγράφηκε: $(10 / 3000)^{-0.2} \approx 3$

Διαγράφηκε: f

Διαγράφηκε: ure

Διαγράφηκε: Gao,

Αλλαγή κωδικού πεδίου

Διαγράφηκε: [

Αλλαγή κωδικού πεδίου

Διαγράφηκε:]

Διαγράφηκε: Crowley

Διαγράφηκε: [

Αλλαγή κωδικού πεδίου

Διαγράφηκε:]

Διαγράφηκε:

Διαγράφηκε: $\Delta t \ll 100$

Διαγράφηκε: $\Delta t \gg 200$

Διαγράφηκε: Δt

Διαγράφηκε: [

Αλλαγή κωδικού πεδίου

Διαγράφηκε:]

Διαγράφηκε: [

Αλλαγή κωδικού πεδίου

Διαγράφηκε:]

Διαγράφηκε: $\xi(q)$

Διαγράφηκε: e

Διαγράφηκε: $K(q)$

Διαγράφηκε: $K(q)$

Διαγράφηκε: Δt

Διαγράφηκε: [

Αλλαγή κωδικού πεδίου

Διαγράφηκε:]

Διαγράφηκε: [

Αλλαγή κωδικού πεδίου

Διαγράφηκε:]

400 In order to quantify this, recall that if the system is linear, the response is a convolution of the system Green's
 401 function with the forcing, in spectral terms it acts as a filter. If it is also scaling, then the filter is a power law: ω^{-H} where ω is the
 402 frequency, (mathematically, if $\widetilde{T(\omega)}$ and $\widetilde{F(\omega)}$ are the Fourier transforms of the response and forcing, for a scaling linear system,
 403 we have: $\widetilde{T(\omega)} \propto \omega^{-H} \widetilde{F(\omega)}$ such a filter corresponds to a fractional integration of order H). In terms of fluctuations this implies:
 404 $\Delta T(\Delta t) = \Delta t^H \Delta F(\Delta t)$ (assuming that the fluctuations are appropriately defined). Therefore, by taking q^{th} powers of both sides and
 405 ensemble averaging, we see that in linear scaling systems we have: $\xi_r(q) = qH + \xi_f(q)$ (c.f. eq. (3) with $\xi_T(q)$ and $\xi_F(q)$ the
 406 structure function exponents for the response and the forcing respectively). If $\xi_r(q)$ and $\xi_f(q)$ only differ by a term linear in q ,
 407 then $K_r(q) = K_f(q)$, so that if over some regime, we find empirically $K_r(q) \neq K_f(q)$ (i.e. the intermitencies are different), then we
 408 may conclude that that the system is nonlinear (note that this result is independent of whether the linearity is deterministic or
 409 only statistical in nature).

410 Let us investigate the nonlinearity of the exponents by returning to Eq. (1), (2) and (3) in more detail. Up until now we
 411 have studied the statistical properties of the forcings and responses using the RMS fluctuations e.g. we have used the following
 412 equation but only for the value $q=2$:

$$\langle \Delta T(\Delta t)^q \rangle \propto \langle \phi_k^q \rangle \Delta t^{qH} = \Delta t^{\xi(q)}; \xi(q) = qH - K(q) \quad (6)$$

413 (see Eq. (1)) the exponent $K(q)$ (implicitly defined in (3)) is given explicitly by:

$$\langle \phi_k^q \rangle = \Delta t^{K(q)}; \frac{\tau_{\text{eff}}}{\Delta t} \quad (7)$$

414 where τ_{eff} is the effective outer scale of the multifractal cascade process, ϕ gives rise to the strong variability and λ' is the
 415 cascade ratio from this outer scale to the scale of interest Δt .

416 If the driving flux ϕ was quasi-Gaussian, then $K(q) = 0$, $\xi(q) = qH$ and the exponent $\xi(2) = 2H = \beta - 1$ would be sufficient
 417 for a complete characterization of the statistics. However geophysical series are often far from Gaussian, even without statistical
 418 analysis, a visual inspection (the sharp spike" of varying amplitudes, see Fig. 1a) of the volcanic series makes it obvious that it is
 419 particularly extreme in this regard. We expect - at least in this case - that the $K(q)$ term will readily be quite large (although note
 420 the constraint $K(1) = 0$ and the mean of ϕ (the $q=1$ statistic) is independent of scale). To characterize this, note that since $K(1) = 0$,
 421 we have $\xi(1) = H$ and then use the first two derivatives of $\xi(q)$ at $q=1$ to estimate the tangent (linear approximation) to $K(q)$ near
 422 the mean (C_1) and the curvature of $K(q)$ near the mean characterized by α . This gives

$$\left. \begin{aligned} (C_1) &= K'(1) = H - \xi'(1) \\ \alpha &= K''(1) / K'(1) = \xi''(1) / (\xi'(1) - H) \end{aligned} \right\} \quad (8)$$

Διαγράφηκε: $\omega^{-H} \dots \widetilde{F(\omega)}$
 $\widetilde{F(\omega)}$... [115]

Διαγράφηκε: and

Διαγράφηκε: $\widetilde{T(\omega)} \propto \omega^{-H} \widetilde{F(\omega)}$

Διαγράφηκε: ,

Διαγράφηκε: $\Delta T(\Delta t) = \Delta t^H \Delta F(\Delta t)$
 $\xi_r(q) = qH + \xi_f(q) \dots \xi_r(q)$
 $\xi_f(q) \dots \xi_r(q) \dots \xi_f(q) \dots$
 $K_r(q) = K_f(q) \dots K_r(q) \neq \dots$ [116]

Διαγράφηκε: $q=2$

Διαγράφηκε: $\langle \Delta T(\Delta t)^q \rangle \propto \langle \phi_k^q \rangle \Delta t^{qH} = \Delta t^{\xi(q)}$
 $\langle \Delta T(\Delta t)^q \rangle \propto \langle \phi_{\lambda'}^q \rangle \Delta t^{\xi(q)}$... [117]

Διαγράφηκε: $K(q)$

Διαγράφηκε: $\langle \phi_{\lambda'}^q \rangle = \Delta t^{K(q)}$

Διαγράφηκε: $\tau_{\text{eff}} \dots \lambda' \dots$
 Δt ... [118]

Διαγράφηκε: $K(q) = 0 \dots$
 $\xi(q) = qH \dots \xi(2) = 2H = \beta$... [119]

Διαγράφηκε: f

Διαγράφηκε: $\text{ure} \dots K(q) \dots$
 $K(1) = 0 \dots q=1 \dots K(1) = 0 \dots \xi(1) = H$
 $\xi(q) \dots q=1 \dots K(q) \dots (C_1)$
 $K(q)$... [120]

Διαγράφηκε: $C_1 = K'(1) = H -$
 $\alpha = K''(1) / K'(1)$

426 The parameters C_1, α are particularly convenient since – thanks to a kind of multiplicative central limit
 427 theorem - there exist multifractal universality classes (Scherzer and Lovejoy, 1987). For such universal multifractal processes,
 428 the exponent function $K(q)$ can be entirely (i.e. not only near $q=1$) characterized by the same two parameters:

429
$$K(q) = \frac{C_1}{\alpha-1} (q^\alpha - q); 0 \leq \alpha \leq 2 \tag{9}$$

430 In the universality case (9), it can be checked that the estimate in (8) (near the mean) is satisfied so that C_1, α
 431 characterize all the statistical moments (actually, (6), (7) are only valid for $q < q_c$; for $q > q_c$, the above will break down due to
 432 multifractal phase transitions; the critical q_c is typically >2 , so that here we confine our analyses to $q \leq 2$ and do not discuss the
 433 corresponding extreme - large q - behaviour).

434 A drawback with using the above fluctuation method for using $\xi(q)$ to estimate $K(q)$ (6) is that if C_1 is not too big, then
 435 for the low order moments q , the exponent $\xi(q)$ may be dominated by the linear (qH) term, so that the multifractal part
 436 ($K(q)$) of the scaling is not too apparent. A simple way of directly studying $K(q)$ is to transform the original series so as to
 437 estimate the flux ϕ at a small scale, essentially removing the (qH) part of the exponent. It can then be degraded by temporal
 438 averaging and the scaling of the various statistical moments - the exponents $K(q)$ - can be estimated directly. To do this, we
 439 divide (1) by its ensemble average so as to estimate the normalized flux at the highest resolution by:

440
$$\phi' = \frac{\phi}{\langle \phi \rangle} = \frac{\Delta T}{\langle \Delta T \rangle} \tag{10}$$

441 where the ensemble average (“ $\langle \rangle$ ”) is estimated by averaging over the available data (here a single series), and the fluctuations
 442 Δt are estimated at the finest resolution (here 1 yr).

444 **4.2 Trace moment analysis of forcings, responses and multiproxies**

445 We now test (7); for convenience, we use the symbol λ as the ratio of a convenient reference scale – here the length of
 446 the series, $\tau_{ref}=1000$ yrs to the resolution scale Δt (for some analyses, 400 yrs was used instead, see the captions in Fig. 6). In an
 447 empirical study, the outer scale τ_{eff} is not known a priori, it must be empirically estimated; denote the scale at which the cascade
 448 starts by λ' .

449 Starting with (7), the basic prediction of multiplicative cascades is that the normalized moments ϕ' (10) obey the generic
 450 multiscaling relation:

451
$$M(q) = \langle \phi'^q \rangle = \lambda'^{K(q)} = \left(\frac{\tau_{eff}}{\Delta t} \right)^{K(q)} = \left(\frac{\lambda}{\lambda_{eff}} \right)^{K(q)}; \lambda' = \frac{\tau_{eff}}{\Delta t} = \frac{\lambda}{\lambda_{eff}}; \lambda_{eff} = \frac{\tau_{ref}}{\tau_{eff}} \tag{11}$$

Διαγράφηκε: C_1, α ... [121]

Διαγράφηκε: [

Διαγράφηκε:]

Αλλαγή κωδικού πεδίου

Διαγράφηκε: $K(q)$... [122]

Διαγράφηκε: $K(q) = \frac{C_1}{\alpha -$

Διαγράφηκε: C_1

$\alpha \dots q < q_c \dots q > q_c \dots q_c \dots$ [123]

Διαγράφηκε: $\xi(q) \dots K(q)$

$C_1 \dots q \dots \xi(q) \dots (qH) \dots (K(q))$

$K(q) \dots \Phi \dots (qH) \dots K(q)$ [124]

Διαγράφηκε: $\phi' = \frac{\phi}{\langle \phi \rangle} = \frac{\Delta T}{\langle \Delta T \rangle}$

Διαγράφηκε: Δt ... [125]

Διαγράφηκε: $\lambda \dots \tau_{ref}=1000 \dots$

Διαγράφηκε: f

Διαγράφηκε: $\tau_{eff} \dots$ [127]

Διαγράφηκε: λ'

Διαγράφηκε: λ_{eff}

Διαγράφηκε: $M(q) = \langle \phi'^q \rangle = \lambda'^{K(q)} = \left(\frac{\tau_{ref}}{\Delta t} \right)^{K(q)} = \left(\frac{\lambda}{\lambda_{eff}} \right)^{K(q)}; \lambda' = \frac{\tau_{ref}}{\Delta t}$

452 We can see that τ_{eff} can readily be empirically estimated since a plot of $\text{Log}_{10}M$ versus $\text{Log}_{10}\lambda$ will have lines
 453 (one for each q , slope $K(q)$) converging at the outer scale $\lambda = \lambda_{eff}$ (although for a single realisation such as here, the outer scale
 454 will be poorly estimated since clearly for a single sample (series) there is no variability at the longest time scales, there is a single
 455 long-term value that generally poorly represents the ensemble mean). Figure 6a shows the results when ΔT is estimated by the
 456 absolute second difference at the finest resolution. The solar forcing (upper right) was only shown for the recent period (1600-
 457 2000) over which the higher resolution sunspot based reconstruction was used, the earlier 1000-1600 part was based on a (too)
 458 low resolution ^{10}Be “splice” as discussed above, see Fig. 2b. In the solar plot (upper left), but especially in the volcanic forcing
 459 plot (upper right), we see that the scaling is excellent over nearly the entire range (the points are nearly linear) and in addition,
 460 the lines plausibly “point” (i.e. cross) at a unique outer scale $\lambda = \lambda_{eff}$ which is not far from the length of the series, see Table 1
 461 for estimates of the corresponding time scales. From these plots we see that the responses to the volcanic forcing “spikiness”
 462 (intermittency) are much stronger than to the corresponding responses to the weaker solar “spikiness”. The model atmosphere
 463 therefore considerably dampens the intermittency, but also this effect is highly nonlinear so that the intermittency of the
 464 combined volcanic and solar forcing (bottom left) is actually a little less than the volcanic only intermittency (bottom right).
 465 Table 1 gives a quantitative characterization of the intermittency strength near the mean, using the C_1 parameter.

466 It is interesting at this stage to compare the intermittency of the ZC outputs with those of the GISS-E2-R GCM (Fig. 6b)
 467 and with multiproxy temperature reconstructions (Fig. 6c). In Fig. 6b, we see that the GISS-E2-R trace moments rapidly die off
 468 at large scales (small λ) so that the intermittency is limited to small scales to the right of the convergence point. In this Figure,
 469 we see that the lines converge at $\text{Log}_{10}\lambda \approx 1.1 - 1.5$ corresponding to τ_{eff} in the range roughly 10–30 yrs. Since the intermittency
 470 builds up scale by scale from large scales modulating smaller scales in a hierarchical manner, and since this range of scales is
 471 small, the intermittency will be small. The partial exception is for the upper right plot which is for the GISS-E2-R response to the
 472 large Gao volcanic forcing (recall that the ZC model uses the weaker, Crowley volcanic reconstruction whose response is
 473 strongly intermittent, see Fig. 6b, the upper left plot). This result shows that contrary to the ZC model whose response is strongly
 474 intermittent (highly non Gaussian) over most of the range of time scales, the GISS-E2-R response is nearly Gaussian implying
 475 that the (highly non Gaussian) forcings are quite heavily (nonlinearly) damped.

476 This difference in the model responses to the forcing intermittency is already interesting, but it does not settle the question
 477 as to which model is more realistic. To attempt to answer this question, we turn to Fig. 6c which shows the trace moment
 478 analysis for six multiproxy temperature reconstructions over the same (pre-industrial) period as the GISS-E2-R model (1500-
 479 1900; unlike the ZC model, the GISS-E2-R included anthropogenic forcings so that the period since 1900 was not used in the
 480 GISS-E2-R analysis). Statistical comparisons of nine multiproxies were made in ch. 11 of Lovejoy and Schertzer, (2013), (for
 481 reasons of space, only six of these are shown in Fig. 6c) where it was found that the pre 2003 multiproxies had significantly
 482 smaller multicentennial and lower frequency variability than the more recent multiproxies used as reference in Fig. 4 and 5.
 483 However, Fig. 6c shows that the intermittencies are all quite low (with the partial exception of the Mann series, see the upper
 484 right plot). This conclusion is supported by the comparison with the red curves. These indicate the generic envelope of trace
 485 moments of quasi-Gaussian processes for $q \leq 2$ it shows how the latter converge (at large scales, small λ , to the left) to the flat

Διαγράφηκε: $\tau_{eff} \dots \log M_e \dots$
 $\log \lambda \dots q \dots K(q) \dots \lambda = \lambda_{eff} \dots$
 ΔT [128]

Διαγράφηκε: f
 Διαγράφηκε: ure...
 $\lambda = \lambda_{eff} \dots t \dots C_1$ [129]

Διαγράφηκε: f
 Διαγράφηκε: ure
 Διαγράφηκε: f
 Διαγράφηκε: ure
 Διαγράφηκε: f
 Διαγράφηκε: ure... [130]
 Διαγράφηκε: f
 Διαγράφηκε: $\log \lambda \approx 1-1.5$
 $\tau_{eff} \dots ca$ [131]
 Διαγράφηκε: f

Διαγράφηκε: f
 Διαγράφηκε: ure... [132]
 Διαγράφηκε: [
 Αλλαγή κωδικού πεδίου
 Διαγράφηκε:]...f [133]
 Διαγράφηκε: ure
 Διαγράφηκε: f
 Διαγράφηκε: ure
 Διαγράφηκε: f
 Διαγράφηκε: ure... [134]

($\kappa(q) = 0$) Gaussian limit. We see that the actual lines are only slightly outside this envelope showing that they are only marginally more variable than quasi-Gaussian processes.

The comparison of the GISS-E2-R outputs (Fig. 6b) with the multiproxies (Fig. 6c) indicates that they are both of low intermittency and are more similar to each other than to the ZC multiproxy statistics. One is therefore tempted to conclude that the GISS-E2-R model is more realistic than the ZC model with its much stronger intermittency. However this conclusion may be premature since the low multiproxy and GISS intermittencies may be due to limitations of both the multiproxies and the GISS-E2-R model. Multicentennial and multimillennial scale ice core analyses displays significant paleotemperature intermittency ($C_i \approx 0.05-0.1$, Schmitt et al., 1995 see the discussion in ch. 11 of Lovejoy and Schertzer, 2013) so that the multiproxies may be insufficiently intermittent.

5. Conclusions

From the point of view of GCM's, climate change is a consequence of changing boundary conditions (including composition), the latter are the climate forcings. Since forcings of interest (such as anthropogenic forcings) are often less than 1% of the mean solar input, the responses are plausibly linear. This justifies the reduction of the forcings to a convenient common denominator: the "equivalent radiative forcing", a concept which is useful only if different forcings add linearly, if they are "additive". An additional consequence of linearity is that the climate sensitivities are independent of whether the fluctuations in the forcings are weak or strong. Both consequences of linearity clearly have their limits. For example, at millennial and longer scales, energy balance models commonly discard linearity altogether and assume that nonlinear albedo responses to orbital changes are dominant. Similarly, at monthly and annual scales, the linearity of the climate sensitivity has been questioned in the context of sharp, strong volcanic forcings.

In view of the widespread use of the linearity assumption, it is important to quantitatively establish its limits and this can best be done using numerical climate models. A particularly convenient context is provided by the Last Millennium simulations, which (in the preindustrial epoch) are primarily driven by the physically distinct solar and volcanic forcings (forcings due to land use changes are very weak). The ideal would be to have a suite of the responses of fully coupled GCM's which include solar only, volcanic only and combined solar and volcanic forcings so that the responses could be evaluated both individually and when combined. Unfortunately, the optimal set of GCM products are the GISS E2-R millennium simulations with solar only and solar plus volcanic forcing (this suite is missing the volcanic only responses). We therefore also considered the outputs of a simplified climate model, the Zebiac-Cane (ZC) model (Mann et al., 2005) for which the full suite was available.

Following a previous study, we first quantified the variability of the forcings as a function of time scale by considering fluctuations. These were estimated by using the difference between the averages of the first and second halves of intervals Δt ("Haar" fluctuations). This definition was necessary in order to capture the two qualitatively different regimes, namely those in which the average fluctuations increase with time scale ($H > 0$) and those in which they decrease with scale ($H < 0$). Whereas the solar forcing was small at annual scales, it generally increased with scale. In comparison, the volcanic forcing was very strong at annual scales but rapidly decreased, the two becoming roughly equal at about 200 yrs. By considering the response to the combined forcing we were then able to examine and quantify their non-additivity (nonlinearity). By direct analysis (Fig. 3b, c), it was found that in the ZC model, additivity of the radiative forcings only works up until roughly 50 yr scales; at 400 yr

Διαγράφηκε: ($\kappa(q) = 0$)

Διαγράφηκε: f

Διαγράφηκε: ure

Διαγράφηκε: f

Διαγράφηκε: ure

Διαγράφηκε: $C_i \approx 0.05-0.1$

Διαγράφηκε: [

Αλλαγή κωδικού πεδίου

Διαγράφηκε:]

Διαγράφηκε: [

Αλλαγή κωδικού πεδίου

Διαγράφηκε:]

Διαγράφηκε: Existing climate models are essentially weather models with extra couplings, coarser resolutions and different parametrizations. Although the models are deterministic, when pushed beyond their predictability limits (≈ 10 days), the high frequency weather acts as a noise so that - following - the overall system can be modelled stochastically. In such approaches, c

Διαγράφηκε: the observed

Διαγράφηκε: relativ[... [135]

Διαγράφηκε:), the [... [136]

Διαγράφηκε: generally

Διαγράφηκε: taken as

Διαγράφηκε: One [... [137]

Διαγράφηκε: thems[... [138]

Διαγράφηκε: One

Διαγράφηκε: In addition

Διαγράφηκε: Simi[... [139]

Διαγράφηκε: [

Διαγράφηκε:]

Διαγράφηκε: $\square t$

Διαγράφηκε: ($H > 0$)

Διαγράφηκε: ($H < 0$)

Διαγράφηκε: f

Διαγράφηκε: ure

Διαγράφηκε: ea

Διαγράφηκε: ea

scales, there are negative feedback interactions between the solar and volcanic forcings that reduce the combined effect by a factor of $\approx 2 - 2.5$. This “subadditivity” makes their combined effects particularly weak at these scales. Although this result seems statistically robust for the ZC Millenium simulations, until the source of the nonlinearity is pin-pointed and the results reproduced with full-blown coupled GCM’s, they must be considered tentative.

In order to investigate possible nonlinear responses to sharp, strong events (such as volcanic eruptions), we used the fact that if the system is linear and scaling, then the difference between the structure function exponents ($\xi(q)$) for the forcings and responses is itself a linear function of the order of moment q (moments with large q are mostly sensitive to the rare large values, small q moments are dominated by the frequent low values). By using the trace moment analysis technique, we isolated the nonlinear part of $\xi(q)$ (i.e. the function $K(q)$) which quantifies the intermittent (multifractal, highly non-Gaussian) part of the variability (associated with the “spikiness” of the signal). Unsurprisingly we showed that the volcanic intermittency was much stronger than the solar intermittency, but that in both cases, the model responses were highly smoothed, they were practically nonintermittent (close to Gaussian) hence that the model responses to sharp, strong events were not characterized by the same sensitivity as to the more common weaker forcing events.

By examining model outputs, we have found evidence that the response of the climate system is reasonably linear with respect to the forcing up to time scales of 50 yrs at least for weak (i.e. not sharp, intermittent) events. But the sharp, intermittent events such as volcanic eruptions that occasionally disrupt the linearity at shorter time scales, become rapidly weaker at longer and longer time scales (with scaling exponent $H \approx -0.3$). In practice, linear stochastic models may therefore be valid from over most of the macroweather range, from ≈ 10 days to over 50 years. However, given their potential importance, it would be worth designing specific coupled climate model experiments in order to investigate this further.

6. Acknowledgements:

The ZC simulation outputs and corresponding solar and volcanic forcings were taken from ftp://ftp.ncdc.noaa.gov/pub/data/paleo/climate_forcing/mann2005/mann2005.txt. We thank J. Lean (solar data [Fig. 2b \(top\)](#), Judith.Lean@nrl.navy.mil), A. Shapiro (solar data, [Fig. 2b \(bottom\)](#)), Alexander Shapiro, alexander.shapiro@pmodwrc.ch) and G. Schmidt (the GISS-E2-R simulation outputs, gavin.a.schmidt@nasa.gov) for graciously providing data and model outputs. The ECHAM5 based Millenium simulations analyzed in table 1 were available from: https://www.dkrz.de/Klimaforschung-en/konsortial-en/millennium-experiments-1?set_language=en. Mathematica and MatLab codes for performing the Haar fluctuation analyses are available from: <http://www.physics.mcgill.ca/~gang/software/index.html>. This work was unfunded, there were no conflicts of interest.

References

- Anderson, J. L.: A method for producing and evaluating probabilistic forecasts from ensemble model integrations, J. Climate, 9, 1518–1530, 1996.
- Ashkenazy, Y., D. Baker, H. Gildor, and Havlin, S.: Nonlinearity and multifractality of climate change in the past 420,000 years. Geophys. Res. Lett., 30, 2146 doi: 10.1029/2003GL018099, 2003.

Διαγράφηκε: ($\xi(q)$)

Διαγράφηκε: q

Διαγράφηκε: q

Διαγράφηκε: q

Διαγράφηκε: $\xi(q)$

Διαγράφηκε: $K(q)$

Διαγράφηκε: ea

Διαγράφηκε: $H \approx -0.3$

Διαγράφηκε: f

Διαγράφηκε: ure

Διαγράφηκε: left

Διαγράφηκε: f

Διαγράφηκε: ure

Διαγράφηκε: right

Διαγράφηκε: 7.

Διαγράφηκε: . (1996),

Διαγράφηκε: .

Διαγράφηκε: S.

Διαγράφηκε: (2003),

Διαγράφηκε: .

- 554 Blender, R., and Fraedrich, K.; Comment on “Volcanic forcing improves atmosphere–ocean coupled general
555 circulation model scaling performance” by D. Vyushin, I. Zhidkov, S. Havlin, A. Bunde, and S. Brenner, *Geophys. Res.
556 Lett.*, 31, L22213, doi: 10.1029/2004GL020797, 2004.
- 557 Bothe, O., Jungclaus, J. H., and Zanchettin, D.; Consistency of the multi-model CMIP5/PMIP3-past1000 ensemble, *Climate of
558 the Past*, 9 (6), 2471–2487, 2013a.
- 559 Bothe, O., Jungclaus, J. H., Zanchettin, D., and Zorita, E.; Climate of the last millennium: Ensemble consistency of simulations
560 and reconstructions, *Climate of the Past*, 9 (3), 1089–1110, 2013b.
- 561 Bryson, R. A.; The Paradigm of Climatology: An Essay, *Bull. Amer. Meteor. Soc.*, 78, 450–456, 1997.
- 562 Budyko, M. I.; The effect of solar radiation variations on the climate of the earth, *Tellus*, 21, 611–619, 1969.
- 563 Bunde, A., Eichner, J. F., Kantelhardt, J. W., and Havlin, S.; Long-term memory: a natural mechanism for the clustering of
564 extreme events and anomalous residual times in climate records, *Phys. Rev. Lett.*, 94, 1–4 doi:
565 10.1103/PhysRevLett.94.048701, 2005.
- 566 Chandra, S., Varotsos, C., and Flynn, L. E.; The mid-latitude total ozone trends in the northern hemisphere, *Geophys Res Lett.*,
567 23(5), 555–558, 1996.
- 568 Clement, A. C., Seager, R., Cane, M. A., and Zebiak, S. E.; An ocean dynamical thermostat, 2190–2196, 1996.
- 569 Crowley, T. J.; Causes of Climate Change Over the Past 1000 Years, *Science*, 289, 270 doi: 10.1126/science.289.5477.270, 2000.
- 570 Dijkstra, H.; *Nonlinear Climate Dynamics*, 357 pp., Cambridge University Press, Cambridge, 2013.
- 571 Eichner, J. F., Koscielny-Bunde, E., Bunde, A., Havlin, S., and Schellnhuber, H.-J.; Power-law persistence and trends in the
572 atmosphere: A detailed study of long temperature records, *Phys. Rev. E*, 68, 046133–046131–046135 doi:
573 10.1103/PhysRevE.68.046133, 2003.
- 574 Fraedrich, K., Blender, R., and Zhu, X.; Continuum Climate Variability: Long-Term Memory, Scaling, and 1/f-Noise,
575 *International Journal of Modern Physics B*, 23, 5403–5416, 2009.
- 576 Franzke, J., Frank, D., Raible, C. C., Esper, J., and Brönnimann, S.; Spectral biases in tree-ring climate proxies *Nature Clim.
577 Change*, 3, 360–364 doi: doi: 10.1038/Nclimate1816, 2013.
- 578 Gao, C. G., Robock, A., and Ammann, C.; Volcanic forcing of climate over the past 1500 years: and improved ice core-based
579 index for climate models, *J. Geophys. Res.*, 113, D23111 doi: 10.1029/2008JD010239, 2008.
- 580 Goswami, B. N., and Shukla, J.; Aperiodic Variability in the Cane—Zebiak Model, *J. of Climate*, 6, 628–638, 1991.
- 581 Hansen, J., Sato, M. K. I., Ruedy, R., Nazarenko, L., Lacis, A., Schmidt, G. A., and Bell, N.; Efficacy of climate forcings, *J.
582 Geophys. Res.*, 110, D18104 doi:10.1029/2005JD005776, 2005.
- 583 Hasselmann, K.; Stochastic Climate models, part I: Theory, *Tellus*, 28, 473–485, 1976.
- 584 Huang, S.; Merging Information from Different Resources for New Insights into Climate Change in the Past and Future,
585 *Geophys. Res. Lett.*, 31, L13205 doi:10.1029/2004 GL019781, 2004.
- 586 Hurst, H. E.; Long-term storage capacity of reservoirs, *Trans. Amer. Soc. Civil Eng.*, 116, 770–808, 1951.
- 587 Huybers, P., and Curry, W.; Links between annual, Milankovitch and continuum temperature variability, *Nature*, 441, 329–332
588 doi:10.1038/nature04745, 2006.
- 589 Kantelhardt, J. W., Koscielny-Bunde, E., Rybski, D., Braun, P., Bunde, A., and Havlin, S.; Long-term persistence and
590 multifractality of precipitation and river runoff record, *J. Geophys. Res.*, 111 doi: doi:10.1029/2005JD005881, 2006.

Διαγράφηκε: K. ...
(2004),.... [140]

Διαγράφηκε: J. H....D. ...n
(2013a),.... [141]

Διαγράφηκε: J. H....D....E.
(2013b), [142]

Διαγράφηκε: (1997),

Διαγράφηκε: (1969),

Διαγράφηκε: J. F....J. W...
S.(2005), [143]

Διαγράφηκε: C. ...L. E...
(1996),.... [144]

Διαγράφηκε: R. ...M. A....S.
E.... (1996),...J. Clin[... [145]

Διαγράφηκε: (2000) [146]

Διαγράφηκε: (2013) [147]

Διαγράφηκε: E....A....S....
H.-J.... (2003),.... [148]

Διαγράφηκε: R....X. ...
(2009),..... [149]

Διαγράφηκε: D. ...C.
C....J.... S.... (2013) [150]

Διαγράφηκε: A. ... C....
(2008)....] Garcia-Serrano, J., and F. J. Doblas-Reyes (2012), On the assessment of near-surface global temperature and North Atlantic multi-decadal variability in the ENSEMBLES decadal hindcast, *Clim. Dyn.*, 39, 2025–2040 doi: DOI 10.1007/s00382-012-1413-1 DEN IPARXEI STO KEIMENO. [151]

Διαγράφηκε: J. ... (1991), [152]

Διαγράφηκε: , et al. (2005)...ear ...doi: [153]

Διαγράφηκε: (1976) [154]

Διαγράφηκε: (2004), ... doi: [155]

Διαγράφηκε: W....(2006), [156]

Διαγράφηκε: E. ...D. ...P.
A. ... S.... (2006),.... [157]

- 591 Kolesnikov, V. N., and [Monin, A. S.](#); Spectra of meteorological field fluctuations, *Izvestiya, Atmospheric and*
592 *Oceanic Physics*, 1, 653-669, [1965](#).
- 593 Kolmogorov, A. N.; A refinement of previous hypotheses concerning the local structure of turbulence in viscous incompressible
594 fluid at high Reynolds number, *Journal of Fluid Mechanics*, 83, 349, [1962](#).
- 595 Kondratyev, K. Y., and [Varotsos, C. A.](#); Volcanic eruptions and global ozone dynamics, *Int. J. Remote Sens.*, 16 (10), 1887-
596 1895, [1995](#).
- 597 Koscielny-Bunde, E., [Bunde, A.](#), [Havlin, S.](#), [Roman, H. E.](#), [Goldreich, Y.](#), and [Schellnhuber, H. J.](#); Indication of a universal
598 persistence law governing atmospheric variability, *Phys. Rev. Lett.*, 81, 729-732, [1998](#).
- 599 Krivova, N. A., [Balmaceda, L.](#), and [Solanki, S. K.](#); Reconstruction of solar total irradiance since 1700 from the surface
600 magnetic field flux, *Astron. and Astrophys.*, 467, 335-346 doi: 10.1051/0004-6361:20066725, [2007](#).
- 601 Laepple, T., [Jewson, S.](#), and [Coughlin, K.](#); Interannual temperature predictions using the CMIP3 multi-model ensemble mean,
602 *Geophys. Res. Lett.*, 35, L17071, doi:10.1029/2008GL033576, 2008.
- 603 Lean, J. L.; Evolution of the Sun's Spectral Irradiance Since the Maunder Minimum, *Geophys. Research Lett.*, 27, 2425-2428,
604 [2000](#).
- 605 Lean, J. L., and [Rind, D. H.](#); How natural and anthropogenic influences alter global and regional surface temperatures: 1889 to
606 2006, *Geophys. Res. Lett.*, 35, L18701 doi: 10.1029/2008GL034864, [2008](#).
- 607 Ljungqvist, F. C.; A new reconstruction of temperature variability in the extra - tropical Northern Hemisphere during the last two
608 millennia, *Geografiska Annaler: Physical Geography*, 92 A(3), 339 - 351 doi:10.1111/j.1468 - 0459.2010.00399.x, [2010](#).
- 609 Lovejoy, S.; What is climate?, *EOS*, 94, (1), 1 January, p1-2, [2013](#).
- 610 Lovejoy, S.; Scaling fluctuation analysis and statistical hypothesis testing of anthropogenic warming, *Climate Dyn.*, 42, 2339-
611 2351 doi:10.1007/s00382-014-2128-2, [2014a](#).
- 612 Lovejoy, S.; A voyage through scales, a missing quadrillion and why the climate is not what you expect, *Climate Dyn.*, 44, 3187-
613 3210, doi: 10.1007/s00382-014-2324-0, [2014b](#).
- 614 Lovejoy, S.; The macroweather to climate transition in the Holocene: regional and epoch to epoch variability (comments on
615 "Are there multiple scaling regimes in Holocene temperature records?" by T. Nilsen, K. Rypdal, and H.-B. Fredriksen),
616 *Earth Syst. Dynam. Discuss.*, 6, C1-C10, [2015a](#).
- 617 Lovejoy, S.; Using scaling for macroweather forecasting including the pause, *Geophys. Res. Lett.*, 42, 7148-7155
618 doi:10.1002/2015GL065665, [2015b](#).
- 619 Lovejoy, S., and [Schertzer, D.](#); Scale invariance in climatological temperatures and the local spectral plateau, *Annales*
620 *Geophysicae*, 4B, 401-410, [1986](#).
- 621 Lovejoy, S., and [Schertzer, D.](#); Towards a new synthesis for atmospheric dynamics: space-time cascades, *Atmos. Res.*, 96, 1-52
622 doi:10.1016/j.atmosres.2010.01.004, [2010](#).
- 623 Lovejoy, S., and [Schertzer, D.](#); Stochastic and scaling climate sensitivities: solar, volcanic and orbital forcings, *Geophys. Res.*
624 *Lett.*, 39, L11702, doi:10.1029/2012GL051871, [2012a](#).
- 625 Lovejoy, S., and [Schertzer, D.](#); Low frequency weather and the emergence of the Climate, in *Extreme Events and Natural*
626 *Hazards: The Complexity Perspective*, edited by A. S. Sharma, A. Bunde, D. N. Baker and V. P. Dimri, pp. 231-254,
627 AGU monographs, Washington D.C., [2012b](#).

Διαγράφηκε: A. S....
(1965),.... [158]

Διαγράφηκε: (1962).... [159]

Διαγράφηκε: C. A. [160]

Διαγράφηκε: A. ...S...H. E.
Y. ... H. J....(1998), [161]

Διαγράφηκε: L.... S.
K....(2007),.... [162]

Διαγράφηκε: S. K....
(2008) [163]

Διαγράφηκε: (2000).... [164]

Διαγράφηκε: D. H. ...
(2008),...ear.... [165]

Διαγράφηκε: (2010).... [166]

Διαγράφηκε: (2013).... [167]

Διαγράφηκε:
(2014a),...amics.... [168]

Διαγράφηκε: (2014).... [169]

Διαγράφηκε:
(2015a),...s..... [170]

Διαγράφηκε: (2015).... [171]

Διαγράφηκε: D. ...
(1986),.... [172]

Διαγράφηκε: ...D. ...
(2010), ...doi: [173]

Διαγράφηκε: D. ... [174]

Διαγράφηκε: doi:
[175]

- 628 Lovejoy, S., and Schertzer, D.: Haar wavelets, fluctuations and structure functions: convenient choices for geophysics,
629 Nonlinear Proc. Geophys., 19, 1-14, doi:10.5194/npg-19-1-2012, 2012c.
- 630 Lovejoy, S., and Schertzer, D.: The Weather and Climate: Emergent Laws and Multifractal Cascades, 496 pp., Cambridge
631 University Press, Cambridge, 2013.
- 632 Lovejoy, S., Schertzer, D., and Varon, D.: Do GCM's predict the climate.... or macroweather?, Earth Syst. Dynam. , 4, 1-16
633 doi:10.5194/esd-4-1-2013, 2013.
- 634 Lovejoy, S., Muller, J. P., and Boisvert, J. P.: On Mars too, expect macroweather, Geophys. Res. Lett., 41, 7694-7700,
635 doi:10.1002/2014GL061861, 2014.
- 636 Lovejoy, S., del Rio Amador, L., and Hébert, R.: The ScaLing Macroweather Model (SLIMM): using scaling to forecast global-
637 scale macroweather from months to Decades, Earth Syst. Dynam., 6, 1-22, doi:10.5194/esd-6-1-2015, 2015.
- 638 Mandelbrot, B. B.: Intermittent turbulence in self-similar cascades: divergence of high moments and dimension of the carrier,
639 Journal of Fluid Mechanics, 62, 331-350, 1974.
- 640 Mann, M. E., Cane, M. A., Zebiak, S. E., and Clement, A.: Volcanic and solar forcing of the tropical pacific over the past 1000
641 years, J. Clim., 18, 447-456, 2005.
- 642 Marzban, C., Wang, R., Kong, F., and Leyton, S.: On the effect of correlations on rank histograms: reliability of temperature and
643 wind speed forecasts from fine scale ensemble reforecasts, Mon. Weather Rev., 139, 295-310,
644 doi:doi:10.1175/2010MWR3129.1, 2011.
- 645 Meehl, G. A., Washington, W. M., Ammann, C. M., Arblaster, J. M., Wigley, T. M. L., and Tebaldi, C.: Combinations Of
646 Natural and Anthropogenic Forcings In Twentieth-Century Climate, J. of Clim. , 17, 3721-3727, 2004.
- 647 Miller, G. H., Geirsdóttir, Á., Zhong, Y., Larsen, D. J., Otto Bliesner, B. L., Holland, M. M., and Anderson, C.: Abrupt onset of
648 the Little Ice Age triggered by volcanism and sustained by sea-ice/ocean feedbacks, Geophys. Res. Lett., 39, L02708
649 doi:10.1029/2011GL050168, 2012.
- 650 Minnis, P., Harrison, E. F., Stowe, L. L., Gibson, G. G., Denn, F. M., Doelling, D. R., and Smith Jr, W. L.: Radiative Climate
651 Forcing by the Mount Pinatubo Eruption, Science, 259 (5100), 1411-1415, 1993.
- 652 Moberg, A., Sonnechkin, D. M., Holmgren, K., Datsenko, N. M., and Karlén, W.: Highly variable Northern Hemisphere
653 temperatures reconstructed from low- and high - resolution proxy data, Nature, 433(7026), 613-617, 2005.
- 654 Newman, M.: An Empirical Benchmark for Decadal Forecasts of Global Surface Temperature Anomalies, J. of Clim., 26, 5260-
655 5269, doi:10.1175/JCLI-D-12-00590.1, 2013.
- 656 Newman, M. P., Sardeshmukh, P. D., and Whitaker, J. S.: A study of subseasonal predictability, Mon. Wea. Rev., 131, 1715-
657 1732, 2003.
- 658 Nicolis, C.: Transient climatic response to increasing CO2 concentration: some dynamical scenarios, Tellus A, 40A, 50-60,
659 doi:10.1111/j.1600-0870.1988.tb00330.x, 1988.
- 660 Østvand, L., Nilsen, T., Rypdal, K., Divine, D., and Rypdal, M.: Long-range memory in millennium-long ESM and AOGCM
661 experiments, Earth System Dynamics, 5, ISSN 2190-4979.s 2295 - 2308.s, doi:10.5194/esd-5-295-2014, 2014.
- 662 Panofsky, H. A., and Van der Hoven, I.: Spectra and cross-spectra of velocity components in the mesometeorological range,
663 Quarterly J. of the Royal Meteorol. Soc., 81, 603-606, 1955.
- 664 Pelletier, J., D.: The power spectral density of atmospheric temperature from scales of 10^{-2} to 10^6 yr, EPSL, 158, 157-164, 1998.
- 665
- 666

Διαγράφηκε: D. (2012c)... [176]

Διαγράφηκε: D.... [177]

Διαγράφηκε: D. ...D. ... (2013),.... [178]

Διαγράφηκε: J. P....J. P.... (2014), [179]

Διαγράφηκε: doi:.. [180]

Διαγράφηκε: L. ...R. ... (2015),.... [181]

Διαγράφηκε: (1974) [182]

Διαγράφηκε: M. A....S. E....A. ... (2005), [183]

Διαγράφηκε: R. F....S.... (2011),.... [184]

Διαγράφηκε: W. M....C. M....J. M. ...T. M. L. C.... (2004),.... [185]

Διαγράφηκε: et al. (2012), doi: [186]

Διαγράφηκε: E. F. ...L. L....G. G. ...F. M. ...D. R. W. L.... (1993),.... [187]

Διαγράφηκε: D. M....K. N. M....W.... (2005), [188]

Διαγράφηκε: (2013), [189]

Διαγράφηκε: P. D.... J. S.... (2003),.... [190]

Διαγράφηκε: (1988), [191]

Διαγράφηκε: doi: [192]

Διαγράφηκε: T. ...K. ...D. M. ... (2014) [191]

Διαγράφηκε: doi:.. [192]

Διαγράφηκε: I. ... ([193]

Διαγράφηκε: (1998), [194]

Διαγράφηκε: **, [194]

- 665 Peng, C.-K., Buldyrev, S. V., Havlin, S., Simons, M., Stanley, H. E., and Goldberger, A. L.: Mosaic organisation of
 666 DNA nucleotides, Phys. Rev. E, 49, 1685-1689, 1994.
- 667 Penland, C., and Sardeshmukh, P. D.: The optimal growth of tropical sea surface temperature anomalies, J. Climate, 8, 1999-
 668 2024, 1995.
- 669 Pielke, R.: Climate prediction as an initial value problem, Bull. of the Amer. Meteor. Soc., 79, 2743-2746, 1998.
- 670 Ragone, F., Lucarini, V., and Lunkeit, F.: A new framework for climate sensitivity and prediction: a modelling perspective,
 671 Climate Dynamics, 1-13, 2014.
- 672 Roques, L., Chekroun, M. D., Cristofol, M., Soubeyrand, S., and Ghi, M.: Parameter estimation for energy balance models with
 673 memory, Proc. Roy. Soc. A, 470 20140349 doi: DOI: 10.1098/rspa.2014.0349, 2014.
- 674 Rybski, D., Bunde, A., Havlin, S., and von Storch, H.: Long-term persistence in climate and the detection problem, Geophys.
 675 Resear. Lett., 33, L06718-06711-06714, doi:10.1029/2005GL025591, 2006.
- 676 Rypdal, M., and Rypdal, K.: Long-memory effects in linear response models of Earth's temperature and implications for future
 677 global warming, J. Climate, 27 (14), 5240 - 5258, doi:10.1175/JCLI-D-13-00296.1, 2014.
- 678 Sardeshmukh, P. D., and Sura, P.: Reconciling non-gaussian climate statistics with linear dynamics, J. of Climate, 22, 1193-
 679 1207, 2009.
- 680 Schertzer, D., and Lovejoy, S.: Physical modeling and Analysis of Rain and Clouds by Anisotropic Scaling of Multiplicative
 681 Processes, Journal of Geophysical Research, 92, 9693-9714, 1987.
- 682 Schmidt, G. A., et al.: Using paleo-climate model/data comparisons to constrain future projections in CMIP5, Clim. Past
 683 Discuss., 9, 775-835, doi:10.5194/cpd-9-775-2013, 2013.
- 684 Schmitt, F., Lovejoy, S., and Schertzer, D.: Multifractal analysis of the Greenland Ice-core project climate data., Geophys. Res.
 685 Lett, 22, 1689-1692, 1995.
- 686 Shackleton, N. J., and Imbrie, J.: The $\delta^{18}O$ spectrum of oceanic deep water over a five-decade band, Climatic Change, 16, 217-
 687 230, 1990.
- 688 Shapiro, A. I., Schmutz, W., Rozanov, E., Schoell, M., Haberreiter, M., Shapiro, A. V., and Nyeki, S.: A new approach to long-
 689 term reconstruction of the solar irradiance leads to large historical solar forcing, Astronomy & Astrophysics, 529, A67,
 690 doi: doi.org/10.1051/0004-6361/201016173, 2011.
- 691 Shindell, D. T., Schmidt, G. A., Miller, R. I., and Mann, M. E.: Volcanic and Solar Forcing of Climate Change during the
 692 Preindustrial Era, J. Clim., 16, 4094-4107, 2003.
- 693 Steinhilber, F., Beer, J., and Frohlich, C.: Total solar irradiance during the Holocene, Geophys. Res. Lett., 36, L19704,
 694 doi:10.1029/2009GL040142, 2009.
- 695 Van der Hoven, I.: Power spectrum of horizontal wind speed in the frequency range from 0.0007 to 900 cycles per hour, Journal
 696 of Meteorology, 14, 160-164, 1957.
- 697 Varotsos, C., Cartalis, C., Vlamakis, A., Tzanis, C. and Keramitsoglou, I.: The long-term coupling between column ozone and
 698 tropopause properties, J Climate, 17(19), 3843-3854, 2004.
- 699 Vyushin, D., Zhidkov, I., Havlin, S., Bunde, A., and Brenner, S.: Volcanic forcing improves atmosphere-ocean coupled, general
 700 circulation model scaling performance. Geophys. Res. Lett., 31, L10206, doi:10.1029/2004GL019499, 2004.
- 701 Wang, Y.-M., Lean, J. L., and Sheeley, N. R. J.: Modeling the Sun's magnetic field and irradiance since 1713, Astrophys J.,
 702 625, 522-538, 2005.

Διαγράφηκε: S. V....S. ...M.
H. E. ...A. L....(1994) (... [195])

Διαγράφηκε: P. D....
(1995), (... [196])

Διαγράφηκε: (1998),

Διαγράφηκε: M.
D....M....S.... M....I (... [197])

Διαγράφηκε: A....S....H....
(2006), (... [198])

Διαγράφηκε: doi:

Διαγράφηκε: K. ... (... [199])

Διαγράφηκε: doi: (... [200])

Διαγράφηκε: P.... (... [201])

Διαγράφηκε: S. ... (... [202])

Διαγράφηκε: doi:

Διαγράφηκε: S. ...D....
(1995), (... [203])

Διαγράφηκε: J. ... (... [204])

Διαγράφηκε: W.... (... [205])

Διαγράφηκε: ... (... [206])

Διαγράφηκε: M....M....A.
V....S.... (2011), (... [207])

Διαγράφηκε: G. A....R.
I....M. E.... (2003), (... [208])

Διαγράφηκε: J. ...C....
(2009), (... [209])

Διαγράφηκε: (1957) (... [210])

Διαγράφηκε: C.
A....C....I.... (2004), (... [211])

Διαγράφηκε: I....S.
A....S.... (2004), (... [212])

Διαγράφηκε: ...do (... [213])

Διαγράφηκε: J. L....N. R.
J.... (2005), (... [214])

- 703 Watson, A. J. and Lovelock, J. E.; Biological homeostasis of the global environment: the parable of Daisyworld,
704 Tellus, 35B, 284-289, 1983.
- 705 Weber, S. L.; A timescale analysis of the Northern Hemisphere temperature response to volcanic and solar forcing, Climate of
706 the Past, 1, 9–17, 2005.
- 707 Zanchettin, D., Rubino, A., and Jungclauss, J. H.; Intermittent multidecadal-to-centennial fluctuations dominate global
708 temperature evolution over the last millennium, Geophys. Res. Lett., 37 (14), L14702, 2010.
- 709 Zanchettin, D., Rubino, A., Matei, D., Bothe, O., and Jungclauss, J. H.; Multidecadal-to-centennial SST variability in the MPI-
710 ESM simulation ensemble for the last millennium, Climate Dynamics, 40 (5-6), 1301-1318, 2013.
- 711 Zebiak, S. E., and Cane, M. A.; A Model El Niño – Southern Oscillation, Mon. Wea. Rev., 115, 2262–2278, 1987.
712 [http://dx.doi.org/10.1175/1520-0493\(1987\)115%3C2262:AMENO%3E2.0.CO;2](http://dx.doi.org/10.1175/1520-0493(1987)115%3C2262:AMENO%3E2.0.CO;2)
- 713 Zhu, X., Fraederich, L., and Blender, R.; Variability regimes of simulated Atlantic MOC, Geophys. Res. Lett., 33, L21603,
714 [doi:10.1029/2006GL027291](https://doi.org/10.1029/2006GL027291), 2006.
- 715
- 716
- Διαγράφηκε: J. E.
 Διαγράφηκε: (1983),
 Διαγράφηκε: (2005),
 Διαγράφηκε: A.
 Διαγράφηκε: J. H.
 Διαγράφηκε: (2010),
 Διαγράφηκε: A.
 Διαγράφηκε: D.
 Διαγράφηκε: O.
 Διαγράφηκε: J. H.
 Διαγράφηκε: (2013)
 Διαγράφηκε: M. A.
 Διαγράφηκε: (1987),
 Διαγράφηκε: doi: doi:
 Διαγράφηκε: .
 Διαγράφηκε: L.
 Διαγράφηκε:
 Διαγράφηκε: R.
 Διαγράφηκε:
 Διαγράφηκε: (2006),
 Διαγράφηκε: 2006.
 Διαγράφηκε: doi:

Tables:

Table 1. The scaling exponent estimates for the forcings and ZC model responses.

	<u>Forcings</u>		<u>Responses</u>			<u>Control Runs</u>	
	<u>Solar</u>	<u>Volcanic</u>	<u>Solar</u>	<u>Volcanic</u>	<u>Combined</u>	<u>GISS</u>	<u>ECHAM5</u>
<u>H</u>	<u>0.40</u>	<u>-0.21</u>	<u>0.031</u>	<u>-0.17</u>	<u>-0.15</u>	<u>-0.26</u>	<u>-0.4</u>
<u>C_1</u>	<u>0.095</u>	<u>0.48</u>	<u>0.022</u>	<u>0.054</u>	<u>0.038</u>	<u><0.01</u>	<u><0.01</u>
<u>α</u>	<u>1.04</u>	<u>0.31</u>	<u>1.82</u>	<u>2.0</u>	<u>2.0</u>	<u>▲</u>	<u>▲</u>
<u>$\xi(2)/2$</u>	<u>0.33</u>	<u>-0.47</u>	<u>-0.01</u>	<u>-0.28</u>	<u>-0.23</u>	<u><0.01</u>	<u><0.01</u>
<u>β</u>	<u>1.66</u>	<u>0.06</u>	<u>0.98</u>	<u>0.44</u>	<u>0.54</u>	<u>0.47</u>	<u>0.2</u>
<u>T_{eff}</u>	<u>630 yrs</u>	<u>300 yrs</u>	<u>100 yrs</u>	<u>100 yrs</u>	<u>250 yrs</u>	<u>▲</u>	<u>▲</u>

Table 1 shows the scaling exponent estimates for the forcings and ZC model responses. For the solar (forcing and response), only the recent 400 yrs (sunspot based) series were used, for the others, the entire 1000 yrs range was used, see figure 6a. The RMS exponent was estimated from Eq. (6), (9): H was estimated from the Haar fluctuations, α , C_1 were estimated from the trace moments (Fig. 6a). Note that the external cascade scales are unreliable since they were estimated from a single realization. The control runs at the right are for the GISS-E2-R model discussed in the text and (ECHAM5) from the fully coupled COSMOS-ASOB Millenium long term simulations based on the Hamburg ECHAM5 model for 800–4000AD.

Μορφοποιήθηκε ... [215]
 Μορφοποιήθηκε ... [216]
 Μορφοποιήθηκε ... [217]
 Μορφοποιήθηκε ... [218]
 Μορφοποιήθηκε ... [219]
 Μορφοποιήθηκε ... [220]
 Μορφοποιήθηκε ... [221]
 Μορφοποιήθηκε ... [222]
 Μορφοποιήθηκε ... [223]
 Μορφοποιήθηκε ... [224]
 Μορφοποιήθηκε ... [225]
 Μορφοποιήθηκε ... [226]
 Μορφοποιήθηκε ... [227]
 Μορφοποιήθηκε ... [228]
 Μορφοποιήθηκε ... [229]
 Μορφοποιήθηκε ... [230]
 Μορφοποιήθηκε ... [231]
 Μορφοποιήθηκε ... [232]
 Μορφοποιήθηκε ... [233]
 Μορφοποιήθηκε ... [234]
 Μορφοποιήθηκε ... [235]
 Μορφοποιήθηκε ... [236]
 Μορφοποιήθηκε ... [237]
 Μορφοποιήθηκε ... [238]
 Μορφοποιήθηκε ... [239]
 Μορφοποιήθηκε ... [240]
 Μορφοποιήθηκε ... [241]
 Μορφοποιήθηκε ... [242]
 Μορφοποιήθηκε ... [243]
 Μορφοποιήθηκε ... [244]
 Μορφοποιήθηκε ... [245]
 Μορφοποιήθηκε ... [246]
 Μορφοποιήθηκε ... [247]
 Μορφοποιήθηκε ... [248]
 Μορφοποιήθηκε ... [249]
 Μορφοποιήθηκε ... [250]
 Μορφοποιήθηκε ... [251]
 Μορφοποιήθηκε ... [252]
 Μορφοποιήθηκε ... [253]
 Μορφοποιήθηκε ... [254]
 Μορφοποιήθηκε ... [255]
 Μορφοποιήθηκε ... [256]
 Μορφοποιήθηκε ... [257]
 Μορφοποιήθηκε ... [258]
 Μορφοποιήθηκε ... [259]
 Μορφοποιήθηκε ... [260]
 Μορφοποιήθηκε ... [261]
 Μορφοποιήθηκε ... [262]
 Μορφοποιήθηκε ... [263]
 Μορφοποιήθηκε ... [264]
 Μορφοποιήθηκε ... [265]
 Μορφοποιήθηκε ... [266]
 Μορφοποιήθηκε ... [267]
 Μορφοποιήθηκε ... [268]
 Μορφοποιήθηκε ... [269]
 Μορφοποιήθηκε ... [270]
 Μορφοποιήθηκε ... [271]
 Μορφοποιήθηκε ... [272]
 Μορφοποιήθηκε ... [273]

Figures and Captions:

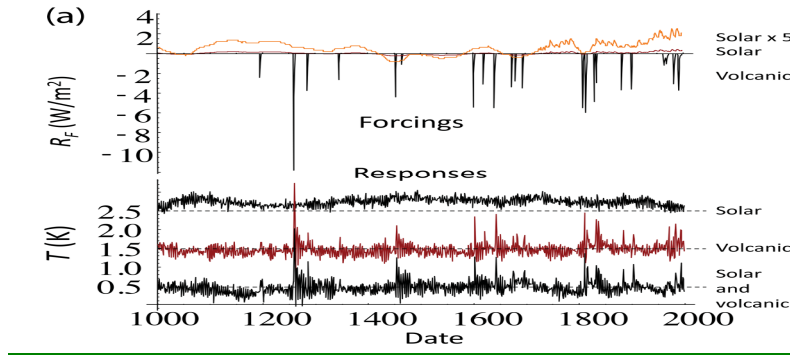


Figure 1a. Top graph: The radiative forcings R_F (top, W/m^2) and responses $T(K)$ from 1000-2000 AD for the Zebiak-Cane model, from Mann et al., (2005), integrated over the entire simulation region. The forcings are reconstructed solar (brown), solar blown up by a factor 5 (orange) and volcanic (red). For the solar forcing (top series), note the higher resolution and wandering character for the recent centuries – this part is based on sunspots, not ^{10}Be . Bottom graph: The responses are for the solar forcing only (top), volcanic forcing only (middle) and both (bottom); they have been offset in the vertical for clarity by 2.5, 1.5, 0.5K respectively.

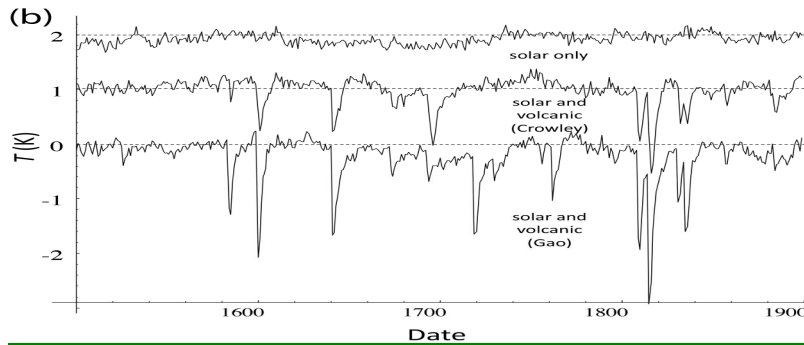


Figure 1b. GISS-ER-2 responses averaged over land, the northern hemisphere at annual resolution. The industrial part since 1900 was excluded due to the dominance of the anthropogenic forcings. The solar forcing is the same as for the ZC model, it is mostly sunspot based (since 1610). The top row is for the solar forcing only, the middle series is the response to the solar and Crowley reconstructed volcanic forcing series (i.e. the same as used in the ZC model); the bottom series uses the solar and reconstructed volcanic forcing series from Gao et al., (2008). Each series has been offset in the vertical by 1K for clarity (these are anomalies so that the absolute temperature values are unimportant).

$R_F (W/m^2)$

$T (K)$

Διανόαφκε:

Αλλαγή κωδικού πεδίου

Διαγράφηκε: [

Αλλαγή κωδικού πεδίου

Διαγράφηκε:]

Διανόαφκε:

$T (K)$

$T (K)$

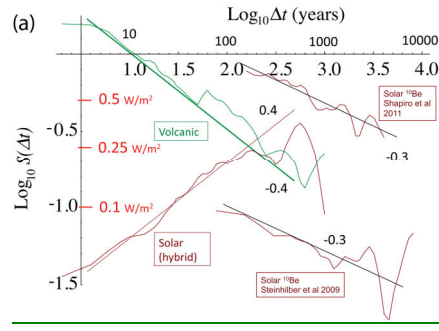
Διαγράφηκε:

Διαγράφηκε: [

Αλλαγή κωδικού πεδίου

Διαγράφηκε:]

743



744

745

746

747

748

749

750

751

Figure 2a. The RMS Haar fluctuation $S(\Delta t)$ for the solar and volcanic reconstructions used in the ZC simulation for lags Δt from 2 to 1000 years (left). The solar is a “hybrid” obtained by “splicing” the sunspot-based reconstruction (Fig. 2b, top) with a ^{10}Be based reconstruction (Fig. 2b, bottom). The two rightmost curves are for two different ^{10}Be reconstructions (Shapiro et al., 2011; Steinhilber et al., 2009). Although at any given scale, their different assumptions lead to amplitudes differing by nearly a factor of 10, their exponents are virtually identical and the amplitudes diminish rapidly with scale.

$\log_{10} S(\Delta t)$

Διανοάφηκε:

Διαγράφηκε: $S(\Delta t)$

Διαγράφηκε: figure

Διαγράφηκε: figure

Διαγράφηκε: [

Αλλαγή κωδικού πεδίου

Διαγράφηκε:]

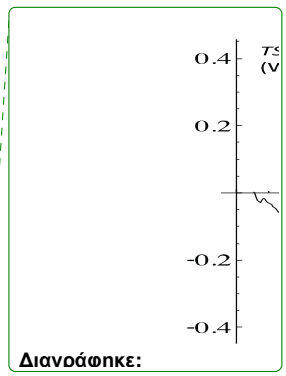
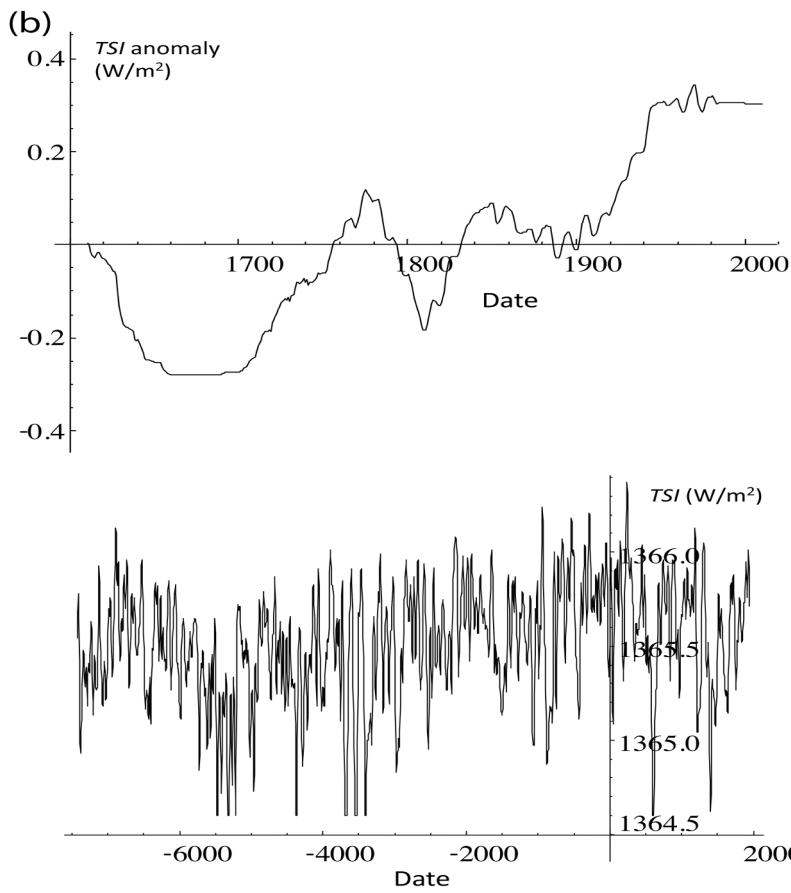
Διαγράφηκε: .

Διαγράφηκε: [

Αλλαγή κωδικού πεδίου

Διαγράφηκε:]

Διαγράφηκε:



752

753

754

755

756

757

758

Figure 2b. A comparison of the sunspot derived Total Solar Irradiance (TSI) anomaly (top, used in the ZC and GISS simulations back to 1610, $H \approx 0.4$) with a recent ^{10}Be reconstruction (bottom, total TSI - mean plus anomaly - since 7362 BC, see Fig. 2a for a fluctuation analysis, $H \approx -0.3$) similar to that “spliced” onto the sunspot reconstruction for the period 1000-1610. We can see that the statistical characteristics are totally different with the sunspot variations “wandering” ($H > 0$) whereas the ^{10}Be reconstruction is “cancelling” ($H < 0$). The sunspot data were for the “background” (i.e. with no 11 year cycle, see Wang et al., 2005 for details), the data for the ^{10}Be curve were from Shapiro et al., (2011).

- Διαγράφηκε: Fig. 2[... [274]
- Διαγράφηκε: $H \approx 0.4$
- Διαγράφηκε: figure
- Διαγράφηκε: $H \approx -0.3$
- Διαγράφηκε: ($H > 0$)
- Διαγράφηκε: ($H < 0$)
- Διαγράφηκε: [
- Αλλαγή κωδικού πεδίου
- Διαγράφηκε:]
- Διαγράφηκε: [
- Αλλαγή κωδικού πεδίου
- Διαγράφηκε:]

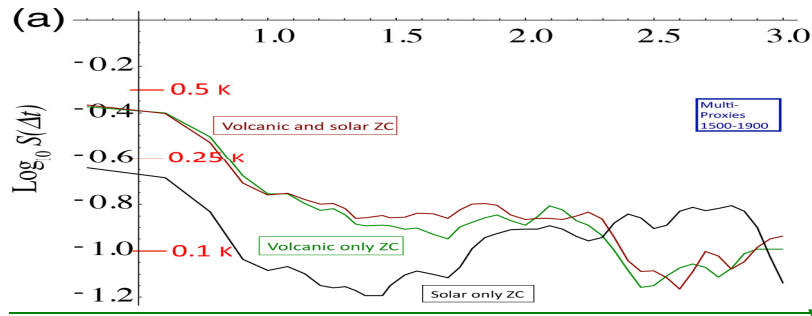


Figure 3a. The RMS Haar fluctuations of the Zebiak–Cane (ZC) model responses (from an ensemble of 100 realizations) with volcanic only (green, from the updated Crowley reconstruction), solar only (black, using the sunspot based background (Wang et al., 2005), and both (brown). No anthropogenic effects were modelled. Also shown for reference are the fluctuations for three multiproxy series (blue, dashed, from 1500-1900, pre-industrial, the fluctuations statistics from the three series were averaged, this curve was taken from Lovejoy and Schertzer, 2012b). We see that all the combined volcanic and solar response of the model reproduces the statistics until scales of ≈ 50 -100 years; however at longer time scales, the model fluctuations are substantially too weak – roughly 0.1K (corresponding to ± 0.05 K) and constant or falling, whereas at 400 yr scales, the temperature fluctuations are ≈ 0.25 K (± 0.125) and rising.

Διαγράφηκε:

Διαγράφηκε: [

Αλλαγή κωδικού πεδίου

Διαγράφηκε:]

Διαγράφηκε: figure 2b left, "spliced" with a ^{10}Be reconstruction with a 40 yr smoother, figure 2b right)

Διαγράφηκε: [

Διαγράφηκε:]

Αλλαγή κωδικού πεδίου

Διαγράφηκε: ea

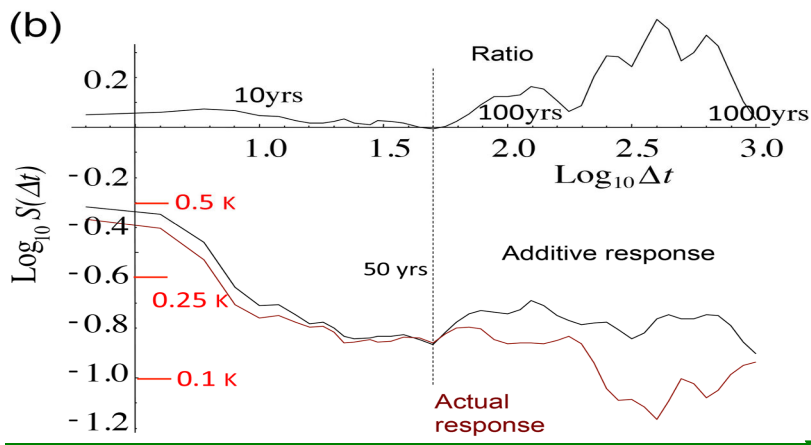


Figure 3b. A comparison of the RMS fluctuations of the ZC model response to combined solar and volcanic forcings (brown, bottom, from Fig. 3a), with the theoretical additive responses (black, bottom) as well as their ratio ($S_{\text{additive}}/S_{\text{actual}}$, black, top). The additive response was determined from the root mean square of the solar only and volcanic only response variances (from Fig. 3a): additivity implies that the fluctuation variances add (assuming that the solar and volcanic forcings are statistically independent). We can see that after about 50 years, there are strong negative feedbacks, the solar and volcanic forcings are subadditive, see Fig. 3c for a blow up of the ratio.

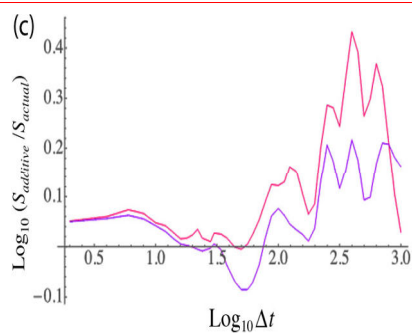


Figure 3c. An enlarged view of the ratio of the linear to nonlinear responses (from Fig. 3b). The top (magenta) curve assumes independence of the solar and volcanic forcings, the bottom purple curve uses the actual response to the combined forcings. The maximum at around 400 yrs (top curve) corresponds to a factor ≈ 2.5 (≈ 1.6 , bottom curve) of negative feedback between the solar and volcanic forcings. The decline at longer durations (Δt 's the single 1000 yr fluctuation) is likely to be an artefact of the limited statistics at these scales.

$$\log_{10} S(\Delta t)$$

Διαγράφηκε:

Διαγράφηκε: figure
 $S_{\text{additive}}/S_{\text{actual}}$... figure (... [275])

$$\log_{10} S_2(\Delta t)$$

0.4

0.3

0.2

0.1

0

-0.1

Διαγράφηκε:

$$\log_{10} (S_{\text{linear}}/S_{\text{actual}})'$$

Διαγράφηκε:

Διαγράφηκε: figure
 ea...ea (... [276])

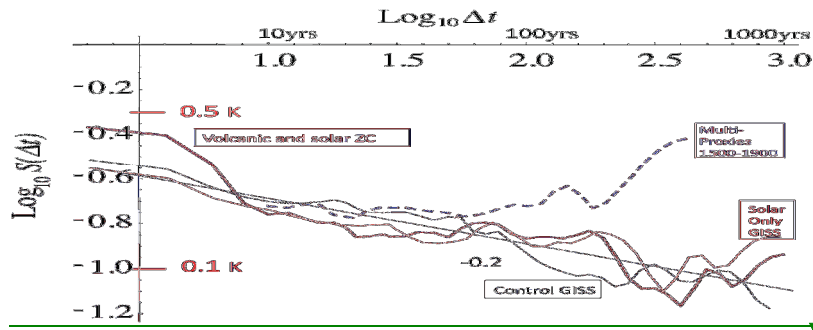


Figure 4. A comparison of the Zebiak-Cane (ZC) model combined (volcanic and solar forcing) response (thick brown) with GISS-E2-R simulations with solar only forcing (red) and a control run (no forcings, black), the GISS structure functions are for land, northern hemisphere, reproduced from Lovejoy et al., (2013).

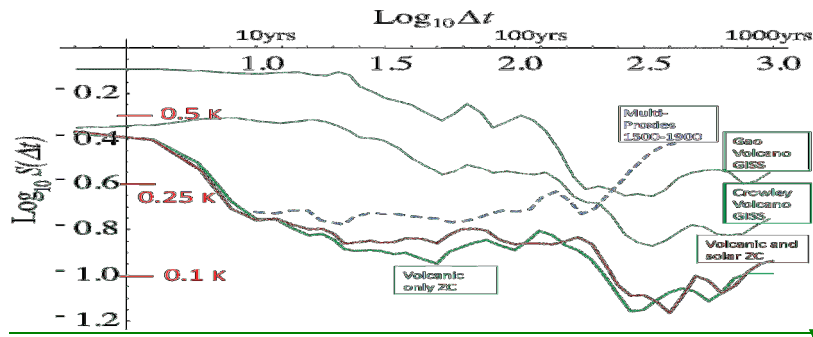
Διανοάφηκε:

Διαγράφηκε: [

Διαγράφηκε:]

Διαγράφηκε: The reference line with slope -0.2 shows the convergence of the control run to the model climate.

Αλλαγή κωδικού πεδίου



Διαγράφηκε:

Διαγράφηκε: Gao,

Διαγράφηκε: [

Αλλαγή κωδικού πεδίου

Διαγράφηκε:]

Διαγράφηκε:)

Διαγράφηκε: [

Διαγράφηκε: Crowley

Αλλαγή κωδικού πεδίου

Διαγράφηκε:]

Διαγράφηκε: [

Αλλαγή κωδικού πεδίου

Διαγράφηκε:]

Figure 5. A comparison of the volcanic forcings for the ZC model (bottom green) and for the GISS-E2-R GCM for two different volcanic reconstructions (Gao et al., 2008, and Crowley, 2000) (top green curves, reproduced from Lovejoy et al., 2013). Also shown is the combined response (ZC, brown) and the preindustrial multiproxies (dashed blue).

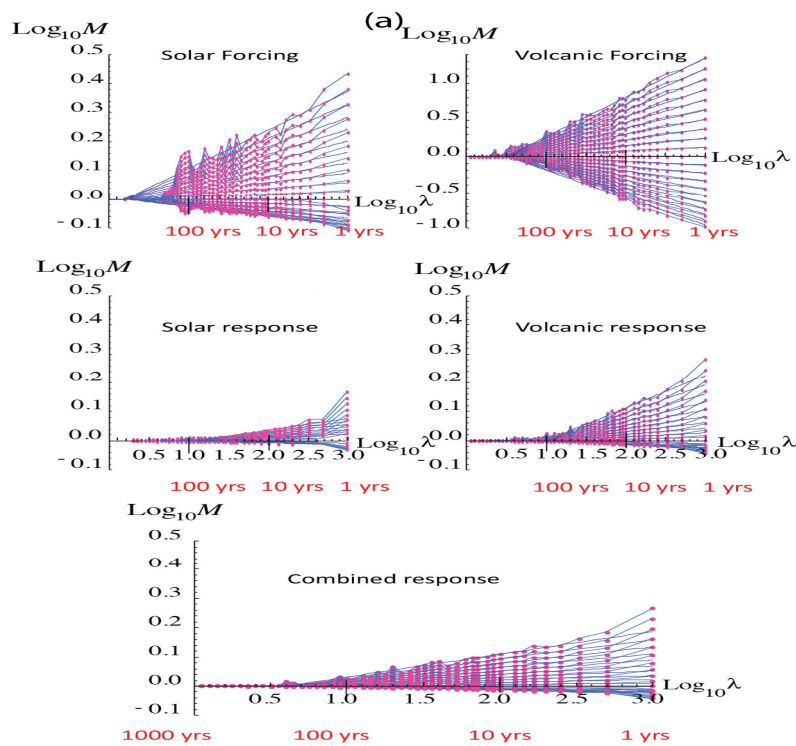


Figure 6a. Analysis of the fluxes/cascade structures of the ZC forcings (top row) and ZC temperature responses (middle, bottom rows); the normalized trace moments (Eq. (11)) are plotted for $q = 2, 1.9, 1.8, 1.7, 1.6, \dots, 0.1$. Upper left is solar forcing (last 400 yrs only, mostly sunspot based), upper right is volcanic, middle left, solar response (last 400 yrs), middle right (volcanic response), lower left, response to combined forcings (last 1000 yrs). Note that all axes are the same except for volcanic. For the solar, only the last 400 yrs were used since this was reconstructed using the more reliable sunspot based method. The earlier ^{10}Be based reconstruction had relatively poor resolution and is not shown. Since the volcanic variability was so dominant, for the combined response (bottom left) the entire series was used. The red points and lines are the empirical values, the blue lines are regressions constrained to go through a single outer scale point. In comparing the different parts of the figure, note in particular i) the log-log linearity for different statistical moments, ii) the fact that the lines for different moments reasonably cross at a single outer scale, and iii) the overall amplitude of the fluctuations – for example by visually comparing the range of the $q = 2$ moments (the top series) as we move from one graph to another.

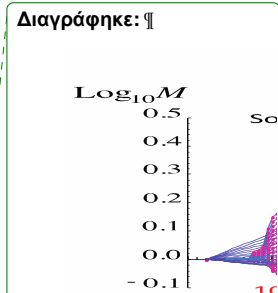


Fig. 6a (top)¶

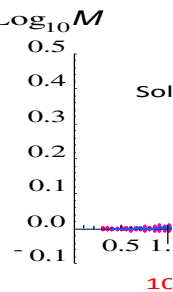


Fig. 6a (middle)¶

... [277]

Διαγράφηκε: e

Διαγράφηκε: ea

Διαγράφηκε: ea

Διαγράφηκε: ea

Διαγράφηκε: at Error!
Objects cannot be created
from editing field codes. , see
(11)

Διαγράφηκε: a

Διαγράφηκε: b

Διαγράφηκε: c